Euro. Jnl of Applied Mathematics (2004), *vol.* 15, *pp.* 1–37.
DOI: 10.1017/S095679250400539X Printed in the United Kingdom

Hele–Shaw flow with a point sink: generic solution breakdown

L. J. CUMMINGS and J. R. KING

School of Mathematics, University of Nottingham, Nottingham NG7 2RD, UK
email: {linda.cummings,john.king}@nottingham.ac.uk

(*Received 28 February 2002; revised 22 May 2003*)

Recent numerical evidence [8, 28, 33] suggests that in the Hele–Shaw suction problem with vanishingly small surface tension γ, the free boundary generically approaches the sink in a wedge-like configuration, blow-up occurring when the wedge apex reaches the sink. Sometimes two or more such wedges approach the sink simultaneously [33]. We construct a family of solutions to the zero-surface tension (ZST) problem in which fluid is injected at the (coincident) apices of an arbitrary number N of identical infinite wedges, of arbitrary angle. The time reversed suction problem then models what is observed numerically with non-zero surface tension. We conjecture that (for a given value of N) a particular member of this family of ZST solutions, with special complex plane singularity structure, is selected in the limit $\gamma \to 0$.

1 Introduction

The numerical solution of the free boundary problem of suction from a point sink in a symmetric fluid domain in a Hele–Shaw cell, with small positive interfacial tension γ, has recently received much attention. In Ceniceros *et al.* [8] and Kelly & Hinch [28], an initially-circular fluid domain is considered, with off-centre suction; while (among other problems) Nie & Tian [33] consider a limacon-shaped fluid domain, with suction from a point on the axis of symmetry. It has long been known that, in the absence of surface tension ($\gamma = 0$), there are simple exact solutions to both these problems [21, 36, 39], which break down in finite time $t^* > 0$ via formation of a 3/2-power cusp in the fluid-air interface. It is anticipated that with $\gamma > 0$ this cuspidal blow-up is circumvented, and the solution can exist beyond time t^*, a conjecture that is supported by the recent numerical simulations of Kelly & Hinch [28], Nie & Tian [33] and Ceniceros *et al.* [8]. More interestingly, in the simulations of Ceniceros *et al.* [8] and Nie & Tian [33], blow-up *does* ultimately occur, but via a different mechanism: the free boundary apparently approaches the sink in the form of a *wedge*, whose apex is ultimately situated at the sink (see Figure 1). (The simulations of Kelly & Hinch [28] also support this theory of the "limiting wedge" configuration, but there the numerics are not carried sufficiently far to be conclusive.) In Ceniceros *et al.* [8], as smaller and smaller values of the surface tension are taken, the wedge angle is seen to approach a definite limit (see Ceniceros *et al.* [8] Table II); moreover, the surface tension values are such that the term the curvature multiplies is

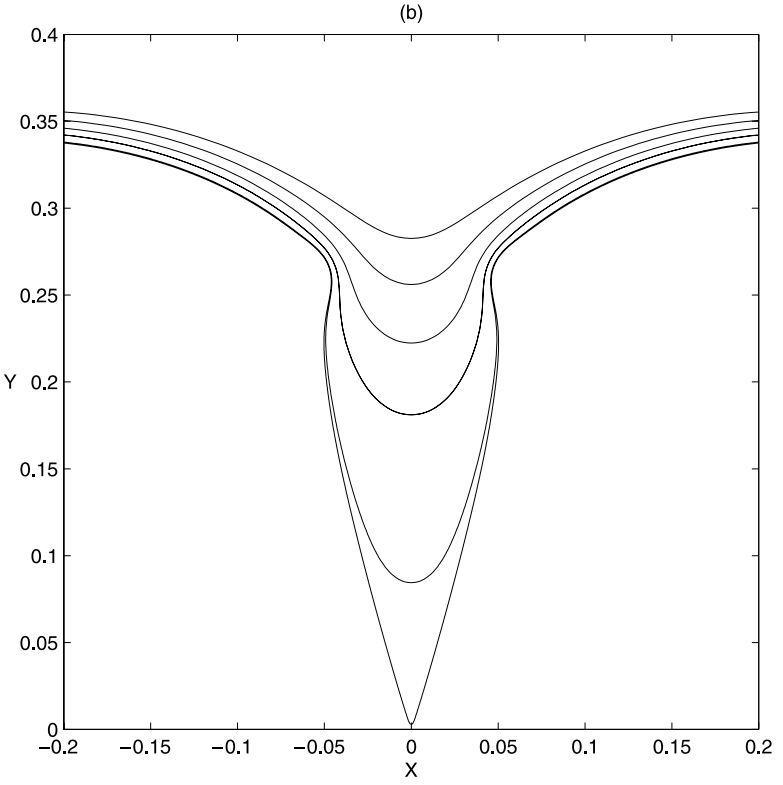

FIGURE 1. Free boundary evolution in the neighbourhood of the sink (situated at $(0,0)$, showing clearly the limiting wedge shape. The dimensionless surface tension coefficient (see § 2) is $\gamma = 5\times10^{-5}$. (Reproduced from Ceniceros *et al.* [8] (Figure 5(b)) by kind permission of the authors.)

apparently negligible during wedge formation, so a zero surface tension theory should be applicable.[1]

Nie & Tian [33] mostly consider the same (small) value for the surface tension throughout, so this 'limiting angle' phenomenon is not observed in Nie & Tian [33]. However, certain solutions of Nie & Tian [33] exhibit the interesting feature of multiple wedge formation, occurring when the initial fluid domain has an axis of symmetry (on which the sink lies). Certain symmetrically-placed points of the boundary move towards the sink faster than other boundary points, and ultimately move in towards the sink as the wedge apices. This phenomenon is also observed in further numerical solutions (by the same authors) of the Hele–Shaw problem driven by a 'multipole' pressure singularity [34]. Here, however, all but one of the computations are carried out for order-one values of the surface tension coefficient, so a ZST theory is not applicable.

[1] There is an interesting (unresolved) issue of what happens as the cusp formation is 'circumvented'. That the small surface tension numerical solution closely approaches the cusped configuration may be seen from Figure 1. This paper is concerned only with the dynamics of the ultimate wedge-type blow-up.

https://doi.org/10.1017/S095679250400539X Published online by Cambridge University Press

The 'selection' of the wedge angle as $\gamma \to 0$ invites the obvious comparison with the Saffman-Taylor fingering problem [42]. Experimentally, an air finger driven along a long rectangular Hele–Shaw channel is seen to occupy a fixed fraction λ of the channel width, which decreases monotonically to one-half as the interfacial tension of the viscous fluid in the cell approaches zero. For the zero-surface tension (ZST) problem, a continuum of solutions exists, giving fingers of any width $\lambda \in (0,1)$. The $\gamma \to 0$ solution is expected to be one member of this family of solutions, but which is actually selected by the regularisation is a delicate problem. The non-zero surface tension (NZST) Hele–Shaw problem is notoriously difficult, and $\gamma > 0$ represents a singular perturbation to the ZST problem for which standard perturbation techniques do not apply due to the ill-posedness of the leading-order problem. The Saffman–Taylor selection problem was finally resolved using exponential asymptotics ('asymptotics beyond all orders') [11, 25, 43]; see also Chapman [9] and Tanveer [46]. Roughly speaking, for all except a discrete spectrum in values of λ, the addition of small positive surface tension to the problem generates (initially exponentially small) perturbations to the solution, which grow unboundedly at large distances from the finger tip.

The Hele–Shaw problem is often treated using a complex variable approach based on the Schwarz function $g(z,t)$ of the free boundary, and the complex potential $w(z,t)$ of the flow; see Howison [27] for an overview.[2] The complex variable z is given by $z = x + iy$, where (x,y) are coordinates in the plane of the cell, and the domain occupied by the fluid in the cell is considered as a domain in the z-plane. An evolution equation relating $g(z,t)$ and $w(z,t)$ may be written down,

$$\frac{\partial w}{\partial z} = \frac{1}{2}\frac{\partial g}{\partial t} + i\gamma \frac{\partial^2}{\partial z^2}\left(\frac{1}{(\partial g/\partial z)^{1/2}}\right), \tag{1.1}$$

from which we see that the $\gamma \to 0$ limit is singular at zeros of $\partial g/\partial z$ in the ZST solution (and also at certain singularities of g). The location of zeros of $\partial g/\partial z$ within the fluid domain, for the family of ZST Saffman–Taylor finger solutions, is closely related to the selection problem. The fluid domain for this family of travelling-wave solutions is described in terms of a conformal map from the unit disc (for example, see Howison [27]):

$$z = f(\zeta,t) = Ut - \frac{1}{\pi}\log\zeta + \frac{2}{\pi}(1-\lambda)\log\left(\frac{1}{2}(1+\zeta)\right) \qquad |\zeta| < 1,$$

where $|\zeta| = 1$ maps to the air-fluid interface and the interval $-1 < \zeta < 0$ along the real axis maps to the channel walls. It is easily shown that the Schwarz function is given in terms of ζ by

$$g(z,t) = G(\zeta,t) = \bar{f}\left(\frac{1}{\zeta},t\right) = Ut - \frac{1}{\pi}(1-2\lambda)\log\zeta + \frac{2}{\pi}(1-\lambda)\log\left(\frac{1}{2}(1+\zeta)\right),$$

where $\bar{f}$ denotes the complex conjugate function, defined by $\bar{f}(\zeta) = \overline{f(\bar{\zeta})}$. Since $\partial g/\partial z = (\partial G/\partial\zeta)/(\partial f/\partial\zeta)$, the zeros of $\partial g/\partial z$ are easily determined. As the finger width λ is varied,

[2] The Schwarz function of an analytic two-dimensional curve $\Gamma(t)$ is the unique function $g(z,t)$, complex analytic in some neighbourhood of $\Gamma(t)$, such that $\bar{z} = g(z,t)$ defines the curve. The complex potential of a Hele–Shaw flow is the complex analytic function $w(z,t)$ whose real part is minus the pressure field.

https://doi.org/10.1017/S095679250400539X Published online by Cambridge University Press

these zeros move in the fluid region ahead of the finger. For $1/2<\lambda<1$ there are two zeros situated symmetrically about the channel centre-line, one on each channel wall, at positions

$$(x_*, y_*) = \left(-\frac{1}{\pi}\log(2\lambda-1) + \frac{2}{\pi}\log(1-\lambda), \pm 1\right)$$

relative to the finger-tip; for $0<\lambda<1/2$ there is a single zero situated on the channel centre-line at position

$$(x_*, y_*) = \left(-\frac{1}{\pi}\log(1-2\lambda) + \frac{2}{\pi}\log(1-\lambda), 0\right)$$

relative to the finger-tip. As λ is decreased from 1, the wall singularities move along the channel walls from $x=-\infty$, $y=\pm 1$, coalescing at $x=+\infty$ on the centre-line when $\lambda=1/2$. As λ then decreases further, the (now simple) zero on the centre-line moves from infinity towards the finger-tip, reaching it when $\lambda=0$. This coalescence of the zeros of g' in the ZST problem is thought to be responsible for the solution selection in the $\gamma\to 0$ problem, and we shall adopt a similar approach to explain the selection of the wedge angle observed in the numerics of Ceniceros *et al.* [8] and Nie & Tian [33].

The rest of this paper is concerned with two distinct, but related, issues. §2–8 are concerned with the problem outlined above, namely the behaviour close to breakdown of the ZST solution selected via the limit $\gamma\to 0$. Motivated by the numerical investigations noted above we first analyse the formation, at time t_w, of an arbitrary number of (symmetrically-placed) ZST free boundary wedges whose apices lies at the sink, and then discuss the selection problem. The limits $\gamma\to 0^+$ and $t\to t_w^-$ do not commute, however, and in §9 we analyse the $t\to t_w^-$ behaviour for arbitrary γ, using the $\gamma\to+\infty$ limit to illustrate the behaviour and noting the (very short) timescale on which such results are pertinent to the $\gamma\to 0$ problem.

2 Overview

The equations and boundary conditions governing Hele–Shaw flow within some region $D(t)$ having free boundary $\partial D(t)$ and a point source (or sink) at the origin are:

$$\nabla^2 p = 0 \quad \text{in } D(t)\backslash\{0\}, \tag{2.1}$$

$$\text{(a)}\quad p=\gamma\kappa, \qquad \text{(b)}\quad \frac{\partial p}{\partial n} = -v_n \quad \text{on } \partial D(t), \tag{2.2}$$

$$p \sim -Q\log r \quad \text{as } r\to 0, \tag{2.3}$$

where p is the pressure within the fluid, κ is the curvature of the free boundary (positive for a convex fluid domain), $\partial/\partial n$ denotes the derivative along the outward normal $\boldsymbol{n}$ to $\partial D(t)$, v_n is the speed of the boundary in this direction, $|Q|$ is the strength of the source or sink and $r=\sqrt{x^2+y^2}$ is the distance from the sink within the fluid. Thus for $\gamma\ll 1$, surface tension is significant in the boundary condition (2.2(a)) only at points of the free boundary where κ is large. For the computations of Ceniceros *et al.* [8] γ is taken so small that the product $\gamma\kappa$ remains small throughout, and in the limit $\gamma\to 0$ its value is

https://doi.org/10.1017/S095679250400539X Published online by Cambridge University Press

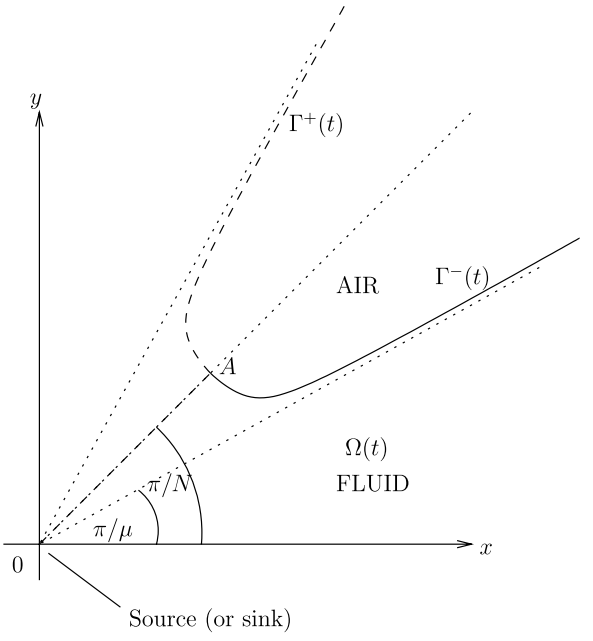

FIGURE 2. The geometry of the problem, showing one portion of the free boundary (half solid line, $\Gamma^-(t)$, half dashed line, $\Gamma^+(t)$) and the line of symmetry $\theta = \pi/N$. Here $N = 4$, so there will be three other identical free boundary portions in the other quadrants. The source of injection is at the origin, and the initial wedge configuration of the free boundary is indicated by dotted lines on either side of the line of symmetry.

significant only at the wedge apex (the sink) at the point of blow-up. Thus we shall seek a suitable family of ZST solutions in the wedge geometry, and use arguments similar to those outlined above to determine which ZST solution is selected in the limit $\gamma \to 0$.

The problem (2.1)–(2.3) with $\gamma = 0$ is easily seen to be time-reversible ($t \mapsto -t$, $p \mapsto -p$), if we also change the sign of the driving singularity Q. We therefore consider the following injection problem and then use time reversal to deduce the local solution we require to the suction problem.

The fluid domain is assumed to have N-fold rotational symmetry, so that successive sectors of angle $2\pi/N$ are identical and N wedges form simultaneously at the blow-up time. The 'fundamental sector' $0 < \theta < 2\pi/N$ (where θ is the usual polar angle) contains, at time $t = 0$, a single wedge of air (symmetric about the line $\theta = \pi/N$) with apex at the origin. Fluid occupies the rest of the sector, initially in two disjoint wedges $0 < \theta < \pi/\mu$, $(2\pi/N - \pi/\mu) < \theta < 2\pi/N$. Thus this sector has reflectional symmetry about the line $\theta = \pi/N$. At time $t = 0^+$ fluid is injected at the origin in accordance with (2.3) ($Q > 0$) and the free boundary advances, the wedge apex moving away from the source as indicated in Figure 2. We must determine the subsequent motion of the free boundary.

Problems in similar geometries have been considered before, notably by King *et al.* [29, 30], Ben Amar & Combescot [2, 3, 13, 14] and Tu [48]; see also [16, 18, 19, 23, 40, 41]. In King *et al.* [29], problems are considered with the same initial geometry as here, but

https://doi.org/10.1017/S095679250400539X Published online by Cambridge University Press

with the flow driven from infinity rather than from the origin; specifically,

$$p \sim \pm r^{\pi/\phi} \cos(\pi\theta/\phi) \qquad \text{as } r \to \infty,$$

(King [30] considers this situation for Hele–Shaw flow with a power-law fluid, and for Stefan problems).

Other papers [2, 3, 13, 14, 48] are concerned with flow in a wedge-shaped Hele–Shaw cell; that is, the wedge sides appear in these problems as rigid, rather than free, boundaries (our problem has only free boundaries). The wedge-shaped cell is filled with fluid initially, and air is then injected, either from the wedge apex, or from infinity, corresponding to a diverging or converging channel. This situation is a direct generalisation of the Saffman-Taylor problem, which is obtained in the limit of zero wedge angle, and has been studied experimentally by Thomé *et al.* [47]. Since we assume rotational and reflectional symmetry, our problem is equivalent to one in a converging channel of angle $2\pi/N$.

Ben Amar [2] derived a family of exact ZST similarity solutions for symmetric 'fingers' in both converging and diverging channels. As with Saffman-Taylor, without surface tension fingers of any angular width exist, but in experiments at small positive surface tension a particular angular width is observed. Using the artifice of a time-dependent flux, which permits self-similar solutions when the surface tension is non-zero, Ben Amar [3] was able to solve the free boundary problem numerically (both converging and diverging channel cases) for small positive surface tension (the smallest dimensionless value computed for was 0.0004). The same problem was addressed analytically (using an 'exponential asymptotics' approach based on the WKB method) by Brener *et al.* [6] (for diverging flows in a Hele–Shaw cell of 90° angle); by Combescot & Ben Amar [13] and Tu [48] (diverging channel of arbitrary angle) and by Combescot [14] (converging and diverging channels, but restricting to small sector angles so that it is close to the classical Saffman–Taylor case). The WKB approach is acknowledged to be non-rigorous, and to lead to only approximate results (see Brener *et al.* [6] and Tu [48], for example). Again, Combescot & Ben Amar [13, 14] use the artifice of time-dependent flux to ensure a self-similar solution with non-zero surface tension, while Brener *et al.* [6] and Tu [48] use a time-dependent surface tension for the same reason.

We note that Tu [48] also presented a family of asymmetric ZST solutions in the wedge geometry, but restricted attention to the symmetric solutions when studying the selection problem. This certainly seems to be the case relevant to the numerics of Ceniceros *et al.* [8] and Nie & Tian [33], and we do likewise.

Much of the work of this paper is closely related to that of Ben Amar [2, 13] and Combescot & Ben Amar [3, 14], but uses different (we believe simpler) methods.

3 Problem formulation: the ZST case

To solve the problem outlined in the previous section, we use a method due to Polubarinova-Kochina [37]. The method (which we shall refer to as the P-K method) was first introduced to solve the rectangular dam problem, but has since been successfully applied to solve a large number of free boundary problems [16, 18, 19, 23, 26, 29]. The current example is a particularly appealing one in that our selection criterion will relate to the complex singularities of the solution, and will therefore rely heavily on the availability

of an explicit conformal mapping solution that determines the behaviour throughout the complex plane. As already mentioned, the ZST solutions we shall use were first given by Ben Amar [2], but we re-derive them here for the reason just given, and because our solution method is quite different.

To get our problem in a form suitable for the application of the technique, we shall make maximum use of symmetry and apply some preliminary transformations. We first note that we need solve the problem only on the sector $0<\theta<\pi/N$, since the 'fundamental sector' $0<\theta<2\pi/N$ has reflectional symmetry about its centreline ($\partial p/\partial\theta=0$ within the fluid on this line). We thus consider the problem on the region $\Omega(t)\subset D(t)$, which we define as the region bounded by the lines $\theta=0$, $\theta=\pi/N$, and $\Gamma^-(t)$ (the lower half of the free boundary as shown in Figure 2). The point A marks the point at which the free boundary intersects the line $\theta=\pi/N$, and is distant $r=R_0$ from the origin.

By the maximum principle for Laplace's equation, the free boundary in a ZST injection problem must be always advancing, hence we can express the free boundary in the form $t=\sigma(\boldsymbol{x})$. We then define the new variable u to be the time integral of the pressure, via the so-called Baiocchi transform, first introduced for the Hele–Shaw problem by Elliott & Janovsky [20] (see also Lacey [31]):

$$u(\boldsymbol{x},t)=u_0(\boldsymbol{x})+\int_0^t p(\boldsymbol{x},\tau)\,d\tau \quad \boldsymbol{x}\in D(0),$$

$$u(\boldsymbol{x},t)=\int_{\sigma(\boldsymbol{x})}^t p(\boldsymbol{x},\tau)\,d\tau \quad \boldsymbol{x}\in D(t)\backslash D(0),$$

(thus $p=\partial u/\partial t$ in $D(t)$) where u_0 satisfies the (ill-posed) Cauchy problem

$$\nabla^2 u_0=1 \quad \boldsymbol{x}\in D(0), \tag{3.1}$$

$$u_0=0=\frac{\partial u_0}{\partial n} \quad \text{on } \partial D(0). \tag{3.2}$$

In the region $|\theta|<\pi/N$ the problem (3.1), (3.2) has solution

$$u_0=\frac{r^2}{2}\sin^2(\pi/\mu-|\theta|),$$

which is singular along $\theta=0$ (the positive x-axis). The singular behaviour of the variable u is then exactly that of u_0, plus the integrals in time of any pressure singularities; and using the definition of u and this fact, u is easily seen to satisfy the following problem on $\Omega(t)$:

$$\nabla^2 u=1 \quad \text{in } \Omega(t), \tag{3.3}$$

$$u=0=\frac{\partial u}{\partial n} \quad \text{on } \Gamma^-(t), \tag{3.4}$$

$$\frac{\partial u}{\partial n}=0 \quad \text{on } \theta=\pi/N,\ 0<r<R_0, \tag{3.5}$$

$$u_y=-\frac{x}{2}\sin(2\pi/\mu) \quad \text{on } \theta=0^+, \tag{3.6}$$

$$u\sim -Qt\log r \quad \text{as } r\to 0, \tag{3.7}$$

$$u\sim\frac{r^2}{2}\sin^2(\pi/\mu-\theta)+k(t)r^{-\mu/2}\cos(\mu\theta/2) \quad \text{as } r\to\infty, \tag{3.8}$$

https://doi.org/10.1017/S095679250400539X Published online by Cambridge University Press

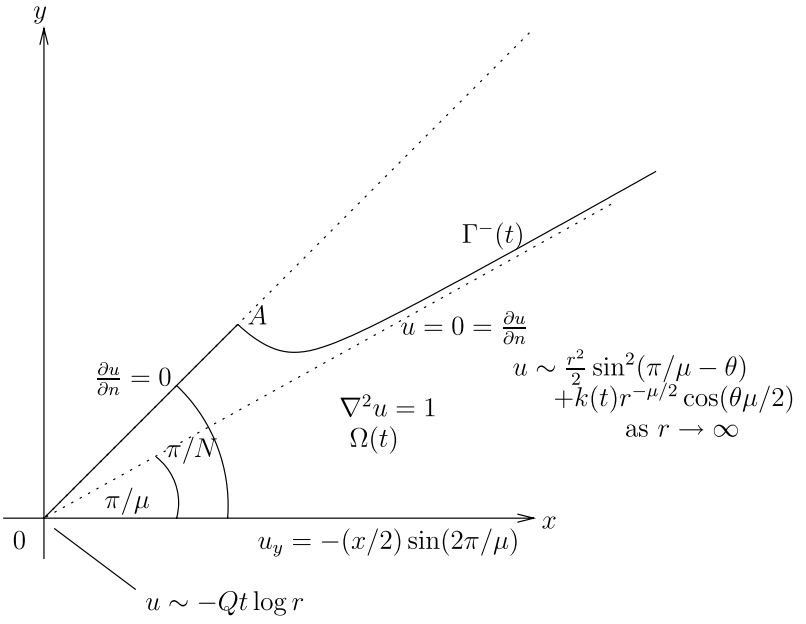

FIGURE 3. The problem for the Baiocchi variable u.

where $k(t)$ is some real but unknown function of time.[3] See Figure 3 for a definition sketch. Following King *et al.* [29], we next introduce the harmonic conjugate pair (Φ, Ψ) and the complex analytic function $W(z)$ by

$$\Phi = u_x - x, \quad \Psi = -u_y, \quad W = \Phi + i\Psi, \tag{3.9}$$

which satisfy the conditions

$$\Psi = \frac{x}{2}\sin(2\pi/\mu) \quad \text{on } \theta = 0^+,$$
$$\Phi = -x, \quad \Psi = 0 \quad \text{on } \Gamma^-(t),$$
$$\sin(\pi/N)(\Phi + x) + \cos(\pi/N)\Psi = 0 \quad \text{on } \theta = \pi/N,\ r < R_0.$$

The fact that the boundary conditions on u reduce to these simple conditions on the real and imaginary parts of the complex analytic function W means that the P-K method is applicable to this problem. The underlying theory is too lengthy to be explained here and we refer elsewhere [15, 37] for details. The method entails expressing the quantities $W = \Phi + i\Psi$ and $z = x + iy$ as analytic functions of an auxiliary complex variable ζ, the physical domain $\Omega(t)$ being mapped into the upper half-plane $\Im(\zeta) > 0$, such that the points $\zeta = \infty$, $\zeta = 0$, $\zeta = 1$ correspond to $z = 0$, $z = \infty$, $z = Z_0 \equiv R_0 \exp(i\pi/N)$, respectively. These three points are the only singular points of the problem, and the P-K theory tells us that the solutions $z = \mathscr{Z}(\zeta)$, $W = \mathscr{W}(\zeta)$ are solutions of a particular hypergeometric

[3] Because the solution to (3.3)–(3.8) is of the self-similar form $u = tU(x/t^{1/2}, y/t^{1/2})$ we know that k is proportional to $t^{1+\mu/4}$.

https://doi.org/10.1017/S095679250400539X Published online by Cambridge University Press

equation, the appropriate one (and the desired solutions) being determined by a local analysis of the behaviour at each of the singular points.

The behaviour of $W(z)$ at the singular points is easily determined from (3.4), (3.5), (3.7), (3.8) and (3.9) as

$$\begin{aligned} W(z) &\sim -\frac{Qt}{z} + (\text{const.}) - \frac{\sin(2\pi/\mu)}{2\pi} z \log z \quad \text{as } z \to 0, \\ W(z) &\sim -z e^{-i\pi/\mu} \cos(\pi/\mu) + \tilde{k}(t) z^{-(1+\mu/2)} \quad \text{as } z \to \infty, \\ W(z) &\sim -X_0 - i e^{-i\pi/N} (z - Z_0) \sin(\pi/N) \quad \text{as } z \to Z_0, \end{aligned}$$

($X_0 = \Re(Z_0)$) and the behaviour of $\mathscr{Z}(\zeta)$ at $\zeta = 0,\ 1,\ \infty$ follows from elementary conformal mappings:

$$\mathscr{Z}(\zeta) \sim A_0(t) e^{i\pi/\mu} \zeta^{-1/\mu} \quad \text{as } \zeta \to 0, \tag{3.10}$$

$$\mathscr{Z}(\zeta) \sim Z_0 - A_1(t) e^{i\pi/N} (\zeta - 1)^{1/2} \quad \text{as } \zeta \to 1, \tag{3.11}$$

$$\mathscr{Z}(\zeta) \sim A_\infty(t) e^{i\pi/N} \left(\frac{1}{\zeta}\right)^{1/N} \quad \text{as } \zeta \to \infty, \tag{3.12}$$

where $A_0(t)$, $A_1(t)$ and $A_\infty(t)$ are unknown real positive functions of time. Hence the behaviour of $\mathscr{W}(\zeta)$ at the singular points is given by:

$$\mathscr{W}(\zeta) \sim -A_0(t) \cos(\pi/\mu) \zeta^{-1/\mu} + O\left(\zeta^{1/2+1/\mu}\right) \quad \text{as } \zeta \to 0, \tag{3.13}$$

$$\mathscr{W}(\zeta) \sim -X_0 + i A_1(t) \sin(\pi/N) (\zeta - 1)^{1/2} \quad \text{as } \zeta \to 1, \tag{3.14}$$

$$\mathscr{W}(\zeta) \sim -\frac{Qt}{A_\infty(t)} e^{-i\pi/N} \left(\frac{1}{\zeta}\right)^{-1/N} \quad \text{as } \zeta \to \infty. \tag{3.15}$$

This local behaviour at the singular points tells us the two *exponents* at each singular point: $(-1/\mu, 1/2 + 1/\mu)$, $(0, 1/2)$, and $(1/N, -1/N)$, at the points 0, 1, ∞, respectively; thus by the P-K theory the solutions $\mathscr{Z}$ and $\mathscr{W}$ are expressible in terms of solutions of the Riemann P-scheme [1, 7, 22] with these exponents. $\mathscr{Z}$ and $\mathscr{W}$ both satisfy the same generalised hypergeometric equation:

$$\frac{d^2u}{d\zeta^2} + \frac{(2\zeta - 1)}{2\zeta(\zeta - 1)} \frac{du}{d\zeta} + \frac{u}{\zeta(\zeta - 1)} \left(\left(\frac{1}{2} + \frac{1}{\mu} \right) \frac{1}{\mu\zeta} - \frac{1}{N^2} \right) = 0; \tag{3.16}$$

we shall use this later. It follows from the theory of Riemann P-functions and hypergeometric functions [1, 7, 22] that $\mathscr{Z}(\zeta)$ and $\mathscr{W}(\zeta)$ are of the form

$$\mathscr{Z}(\zeta) = \zeta^{-1/\mu} (D_1 U(\zeta) + D_2 V(\zeta)), \tag{3.17}$$

$$\mathscr{W}(\zeta) = \zeta^{-1/\mu} (E_1 U(\zeta) + E_2 V(\zeta)), \tag{3.18}$$

where D_j, E_j are time-dependent complex coefficients, and U and V are linearly independent solutions of the hypergeometric equation

$$\zeta(1 - \zeta) \frac{d^2u}{d\zeta^2} + \left(\frac{1}{2} - \frac{2}{\mu} - \left(1 - \frac{2}{\mu} \right) \zeta \right) \frac{du}{d\zeta} + \left(\frac{1}{N^2} - \frac{1}{\mu^2} \right) u = 0. \tag{3.19}$$

https://doi.org/10.1017/S095679250400539X Published online by Cambridge University Press

We take $U(\zeta)$ to be the standardised hypergeometric function (uniformly convergent on the unit disc)

$$U(\zeta) = F\left(\frac{1}{N} - \frac{1}{\mu}, -\frac{1}{N} - \frac{1}{\mu}; \frac{1}{2} - \frac{2}{\mu}; \zeta\right), \tag{3.20}$$

and $V(\zeta)$ to be the solution of (3.19) defined by

$$V(\zeta) = \zeta^{-\frac{1}{N}+\frac{1}{\mu}} F\left(\frac{1}{N} - \frac{1}{\mu}, \frac{1}{2} + \frac{1}{N} + \frac{1}{\mu}; 1 + \frac{2}{N}; \zeta^{-1}\right) \tag{3.21}$$

(uniformly convergent *outside* the unit disc; this choice turns out to be convenient for matching the behaviours at $\zeta = \infty$). The coefficients D_j and E_j are determined by matching the behaviour in (3.10)–(3.15) to that of (3.17) and (3.18) at the singular points. The behaviour of $U(\zeta)$ at $\zeta = 0$, and of $V(\zeta)$ near $\zeta = \infty$, is given by the standard hypergeometric series [1, 7, 22], and the behaviour of $U(V)$ at $\zeta = 1$ and $\zeta = \infty$ ($\zeta = 0$) may be deduced using functional identities given in Abramowitz & Stegun [1] and Gradshteyn & Ryzhik [22].

Matching the singular behaviour at $\zeta = \infty$ gives

$$D_1 = 0, \qquad D_2 = A_\infty e^{i\pi/N},$$
$$E_2 e^{\pm i\pi(1/N+1/\mu)} \frac{\Gamma\left(\frac{1}{2} - \frac{2}{\mu}\right)\Gamma\left(\frac{2}{N}\right)}{\Gamma\left(\frac{1}{N} - \frac{1}{\mu}\right)\Gamma\left(\frac{1}{2} + \frac{1}{N} - \frac{1}{\mu}\right)} = -\frac{Qt}{A_\infty} e^{-i\pi/N};$$

matching the behaviour at $\zeta = 0$ gives

$$D_2 \frac{\Gamma\left(1 + \frac{2}{N}\right)\Gamma\left(\frac{1}{2} + \frac{2}{\mu}\right)}{\Gamma\left(\frac{1}{2} + \frac{1}{N} + \frac{1}{\mu}\right)\Gamma\left(1 + \frac{1}{N} + \frac{1}{\mu}\right)} e^{\pm i\pi(1/N-1/\mu)} = A_0 e^{i\pi/\mu},$$
$$E_1 + E_2 \frac{\Gamma\left(1 + \frac{2}{N}\right)\Gamma\left(\frac{1}{2} + \frac{2}{\mu}\right)}{\Gamma\left(\frac{1}{2} + \frac{1}{N} + \frac{1}{\mu}\right)\Gamma\left(1 + \frac{1}{N} + \frac{1}{\mu}\right)} e^{\pm i\pi(1/N-1/\mu)} = -A_0 \cos(\pi/\mu);$$

and finally, matching the behaviour at $\zeta = 1$ (the terms of order 1 and $(1-\zeta)^{1/2}$ must both be matched) gives

$$Z_0 \equiv R_0 e^{i\pi/N} = D_2 \frac{\Gamma\left(1 + \frac{2}{N}\right)\Gamma\left(\frac{1}{2}\right)}{\Gamma\left(1 + \frac{1}{N} + \frac{1}{\mu}\right)\Gamma\left(\frac{1}{2} + \frac{1}{N} - \frac{1}{\mu}\right)},$$
$$-A_1 e^{i\pi/N} = D_2 \frac{\Gamma\left(1 + \frac{2}{N}\right)\Gamma\left(-\frac{1}{2}\right)}{\Gamma\left(\frac{1}{N} - \frac{1}{\mu}\right)\Gamma\left(\frac{1}{2} + \frac{1}{N} + \frac{1}{\mu}\right)},$$
$$-X_0 = E_1 \frac{\Gamma\left(\frac{1}{2} - \frac{2}{\mu}\right)\Gamma\left(\frac{1}{2}\right)}{\Gamma\left(\frac{1}{2} - \frac{1}{N} - \frac{1}{\mu}\right)\Gamma\left(\frac{1}{2} + \frac{1}{N} - \frac{1}{\mu}\right)} + E_2 \frac{\Gamma\left(1 + \frac{2}{N}\right)\Gamma\left(\frac{1}{2}\right)}{\Gamma\left(1 + \frac{1}{N} + \frac{1}{\mu}\right)\Gamma\left(\frac{1}{2} + \frac{1}{N} - \frac{1}{\mu}\right)},$$
$$e^{i\pi/2} A_1 \sin(\pi/N) = E_1 e^{\pm i\pi/2} \frac{\Gamma\left(\frac{1}{2} - \frac{2}{\mu}\right)\Gamma\left(-\frac{1}{2}\right)}{\Gamma\left(\frac{1}{N} - \frac{1}{\mu}\right)\Gamma\left(-\frac{1}{N} - \frac{1}{\mu}\right)} + E_2 \frac{\Gamma\left(1 + \frac{2}{N}\right)\Gamma\left(-\frac{1}{2}\right)}{\Gamma\left(\frac{1}{N} - \frac{1}{\mu}\right)\Gamma\left(\frac{1}{2} + \frac{1}{N} + \frac{1}{\mu}\right)}.$$

We find that these conditions can be satisfied simultaneously only for a particular choice of the signs, giving a unique solution for $\mathscr{Z}(\zeta)$ and $\mathscr{W}(\zeta)$. We give only the final solution

https://doi.org/10.1017/S095679250400539X Published online by Cambridge University Press

for $\mathscr{Z}(\zeta)$, since we are primarily interested in the free boundary evolution. In $|\zeta|>1$ this is

$$\mathscr{Z}(\zeta)=A_\infty e^{i\pi/N}\zeta^{-1/N}F\left(\frac{1}{N}-\frac{1}{\mu},\frac{1}{2}+\frac{1}{N}+\frac{1}{\mu};1+\frac{2}{N};\zeta^{-1}\right),$$
$$A_\infty=\frac{\left(QNt\Gamma\left(\frac{2}{N}-\frac{2}{\mu}\right)\Gamma\left(1+\frac{2}{N}+\frac{2}{\mu}\right)\right)^{1/2}}{2^{2/N}\Gamma\left(\frac{2}{N}\right)}. \tag{3.22}$$

To plot the free boundary evolution we need the form of the solution valid in $|\zeta|\leqslant 1$. Provided $\frac{1}{2}+\frac{2}{\mu}$ is not an integer this expression is given by

$$\mathscr{Z}(\zeta)=\Lambda\left\{\frac{\Gamma\left(\frac{1}{2}+\frac{2}{\mu}\right)e^{i\pi/\mu}\zeta^{-1/\mu}}{\Gamma\left(\frac{1}{2}+\frac{1}{N}+\frac{1}{\mu}\right)\Gamma\left(1+\frac{1}{N}+\frac{1}{\mu}\right)}F\left(\frac{1}{N}-\frac{1}{\mu},-\frac{1}{N}-\frac{1}{\mu};\frac{1}{2}-\frac{2}{\mu};\zeta\right)\right.$$
$$\left.-i\frac{\Gamma\left(-\frac{1}{2}-\frac{2}{\mu}\right)e^{-i\pi/\mu}\zeta^{1/2+1/\mu}}{\Gamma\left(\frac{1}{N}-\frac{1}{\mu}\right)\Gamma\left(\frac{1}{2}+\frac{1}{N}-\frac{1}{\mu}\right)}F\left(\frac{1}{2}+\frac{1}{N}+\frac{1}{\mu},\frac{1}{2}-\frac{1}{N}+\frac{1}{\mu};\frac{3}{2}+\frac{2}{\mu};\zeta\right)\right\}, \tag{3.23}$$

(see formula 15.3.7 in [1]; this is uniformly convergent on the unit disc) where

$$\Lambda=2^{1-2/N}\left(\frac{Qt}{N}\Gamma\left(\frac{2}{N}-\frac{2}{\mu}\right)\Gamma\left(1+\frac{2}{N}+\frac{2}{\mu}\right)\right)^{1/2}. \tag{3.24}$$

If $\frac{1}{2}+\frac{2}{\mu}=n\in\mathbb{N}$, however, both terms in this expression are singular (the first hypergeometric function, and the Gamma-function premultiplying the second hypergeometric function). Bearing in mind that $\mu>N$ (so $\mu>1$ always) this can occur only for $n=1$ (with $\mu=4$ and $N=1$, 2 or 3) or for $n=2$ (with $\mu=4/3$ and $N=1$). The expression for $Z(\zeta)$ valid in $|\zeta|>1$ for these four cases is given in Appendix A.

The free boundary portion $\Gamma^-(t)$ is the image of $\zeta=\xi\in(0,1)$ on the real positive ζ-axis: $x(\xi)+iy(\xi)=\mathscr{Z}(\xi)$, and from (3.23) can be seen to move in a self-similar manner. Thus, we have an exact solution to the ZST free boundary problem for any values of N and μ, excepting those listed above. As written above, the solution pertains to the injection problem in which the initial configuration is N fluid wedges separated by N air wedges. The free boundary evolution for the corresponding suction problem is easily obtained by replacing t by (t_w-t) in the expression for $\mathscr{Z}(\zeta)$ (and Q by $|Q|$ if one assumes $Q<0$ for a point sink).

Note that the map to the entire fluid sector $0<\theta<2\pi/N$ is given by the combined mapping from the entire ζ-plane, slit along $[0,1]$:

$$\Sigma(\zeta)=\begin{cases}\mathscr{Z}(\zeta) & \Im(\zeta)>0,\\ e^{2\pi i/N}\bar{\mathscr{Z}}(\zeta) & \Im(\zeta)<0.\end{cases} \tag{3.25}$$

(The function Σ is analytic on the slit ζ-plane, because $\mathscr{Z}$ and $\bar{\mathscr{Z}}$ are analytic on the upper- and lower-half ζ-planes respectively, and for $\xi\in\mathbb{R}$ it is easily checked that $\mathscr{Z}(\xi)=e^{2\pi i/N}\bar{\mathscr{Z}}(\xi)$ for $\xi>1$ and $\xi<0$.) The upper side of the slit maps to $\Gamma^-(t)$ and the lower side to $\Gamma^+(t)$.

Figures 4 ($N=1$), 5 ($N=2$) and 6 ($N=3$) show the evolution of the free boundary from the initial wedge configuration for the critical values of μ found below (evolution from different angled wedges is qualitatively similar).

https://doi.org/10.1017/S095679250400539X Published online by Cambridge University Press

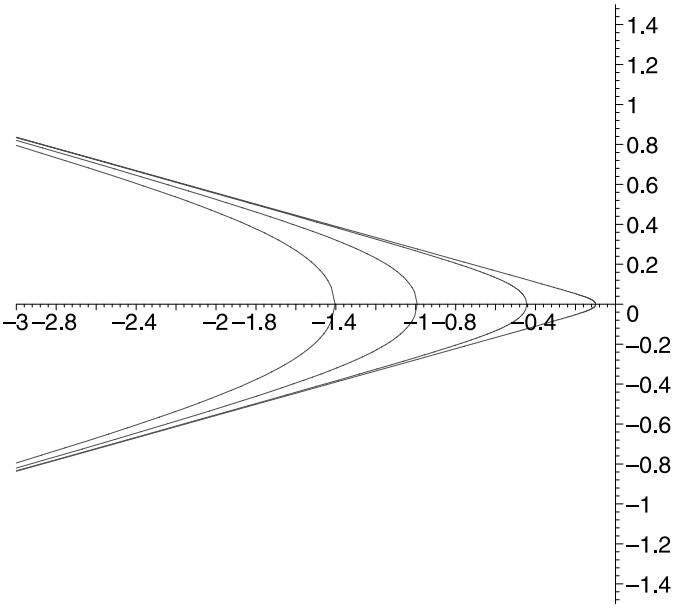

FIGURE 4. The free boundary evolution for the critical angle solution $N = 1$, $\mu_* \approx 1.09473$. The angle of the air-wedge is given by $2\pi(1 - 1/\mu_*)$. The times shown are $(t_w - t) = 0.2$, $(t_w - t) = 0.1$, $(t_w - t) = 0.02$, $(t_w - t) = 0.001$.

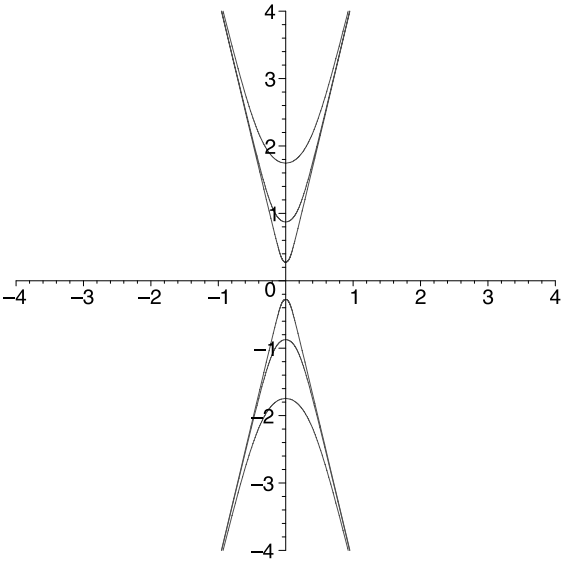

FIGURE 5. The free boundary evolution for the critical angle solution $N = 2$, $\mu_* \approx 2.34966$. The angle of the air-wedge is given by $2\pi(1/2 - 1/\mu_*)$. The times shown are $(t_w - t) = 0.4$, $(t_w - t) = 0.1$, $(t_w - t) = 0.01$.

https://doi.org/10.1017/S095679250400539X Published online by Cambridge University Press

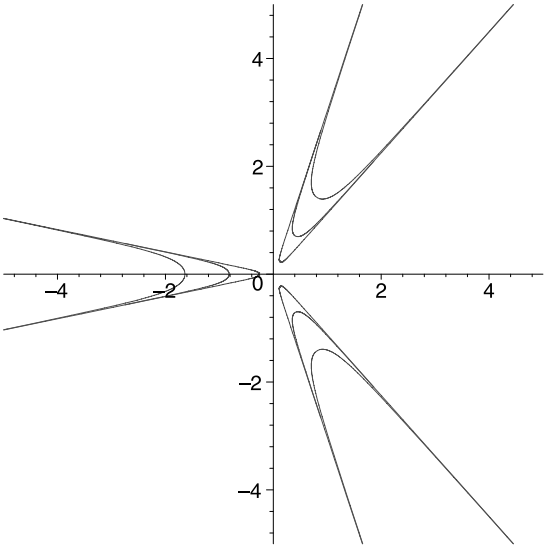

FIGURE 6. The free boundary evolution for the critical angle solution $N=3$, $\mu_* \approx 3.72692$. The angle of the air-wedge is given by $2\pi(1/3-1/\mu_*)$. The times shown are $(t_w-t)=0.4$, $(t_w-t)=0.1$, $(t_w-t)=0.01$.

4 The selection problem: General theory

4.1 Preamble

We turn now to the problem with small positive surface tension, and address the question of which of the family of zero-surface tension (ZST) solutions found above is selected in the limit as the surface tension goes to zero. The selection mechanism proposed is remarkably simple and quite general. We use the Schwarz function approach mentioned in the Introduction. Recall that the Schwarz function $g(z,t)$ of a two-dimensional analytic curve $\Gamma(t)$ is the unique complex function, analytic in some neighbourhood of $\Gamma(t)$, such that $\bar{z}=g(z,t)$ defines $\Gamma(t)$. It is related to the complex potential by equation (1.1). The utility of this equation lies in our knowledge that, in the absence of driving singularities, the complex potential w must be analytic throughout the flow domain $\Omega(t)$, as its real and imaginary parts represent physical quantities. Thus, while ZST solutions admit zeros in the derivative of g at (moving) points $z=z_*(t)$ within the physical domain, NZST solutions do not. This is easily demonstrated, since such a zero would give a singularity on the right-hand side, requiring a singularity in $\partial g/\partial t$ to cancel it. Suppose $\partial g/\partial z(z_*(t),t)=0$, then $\partial^2 g/\partial t\partial z$ cannot be infinite (except possibly at a single instant) at $z=z_*(t)$. If we differentiate equation (1.1) with respect to z, then the requirement that $\partial^2 w/\partial z^2$ be analytic in Ω means that

$$\frac{\partial^2 g}{\partial t\partial z}+2i\gamma\frac{\partial^3}{\partial z^3}\left(\frac{1}{(\partial g/\partial z)^{1/2}}\right)=\{\text{analytic near } z=z_*(t)\}.$$

Given this observation, $\partial^2 g/\partial t\partial z$ cannot balance the singular term $\partial^3/\partial z^2(1/\sqrt{g'(z,t)})$, and so this requirement cannot be fulfilled. Hence zeros of $g'(z,t)$ are not permissible in the NZST problem.

https://doi.org/10.1017/S095679250400539X Published online by Cambridge University Press

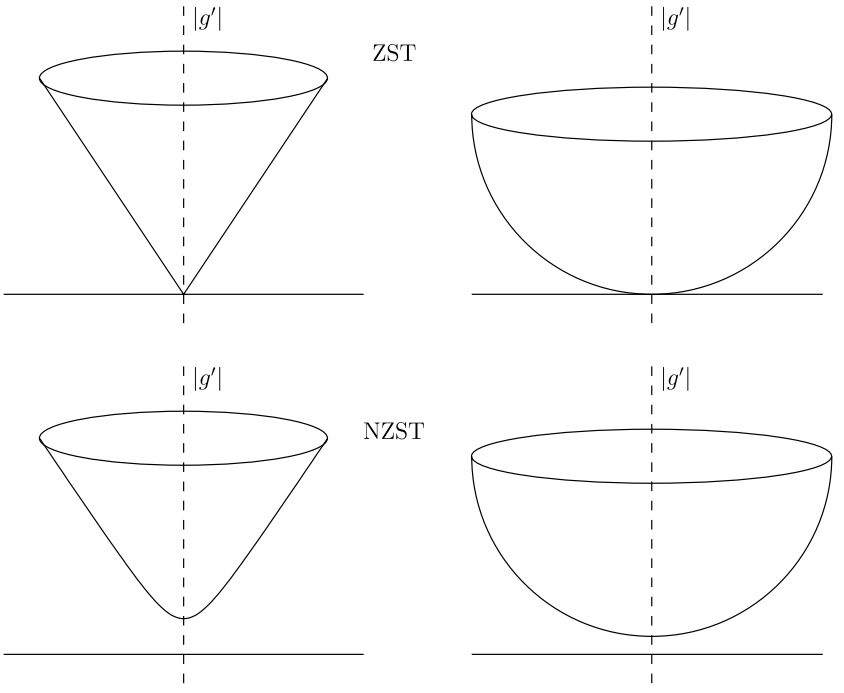

FIGURE 7. The two possibilities for the behaviour of $|g'|$ as γ increases from zero, in the neighbourhood of a point where the ZST g' has a zero.

In general, however, ZST Hele-Shaw solutions are such that $g'(z,t)$ has zeros on $\Omega(t)$. Considering $|g'(z,t)|$ as a real-valued function of (x,y) in the neighbourhood of such a zero, there are two possibilities: either (I) the surface at height $|g'(z,t)|$ above the z-plane (or (x,y)-plane) is locally conical, i.e. the zero of g' is simple, or (II) it is locally bowl-like, i.e. the zero of g' is repeated (see the upper ZST pictures in Figure 7). We wish to know which, from the available family of ZST solutions, is selected in the limit $\gamma \to 0$. Figure 7 shows the situation for $0 < \gamma \ll 1$ in each of cases I and II. In either case there can no longer be a zero in g' by the argument above. In case I some local smoothing of the surface is necessary, since otherwise the cone apex (now at nonzero height) would represent a singularity in g'', which again cannot be reconciled with (1.1). No such smoothing is needed in case II. In each of cases I and II we may attempt an asymptotic expansion of the Schwarz function in a neighbourhood of the ZST zero of g', $z = z_*(t)$ say, as $\gamma \to 0$. We write $\tilde{z} = z - z_*(t)$, $T = t$ and $\tilde{z} = \delta Z$ (where δ, the size of the inner region, is to be determined and will be different in the two cases), and $h = g'$ (equation (1.1) differentiated once with respect to z gives an equation for h).

In case I the behaviour as $\tilde{z} \to 0$ is $h \sim a(T)\tilde{z} + O(\tilde{z}^2)$ (simple zero), while in case II we have $h \sim b(T)\tilde{z}^2 + O(\tilde{z}^3)$ (repeated zero), where a and b are complex functions of time, suggesting that in the inner we write

$$h = \delta_{\mathrm{I}} H \text{ (case I)}, \quad h = \delta_{\mathrm{II}}^2 H \text{ (case II)}. \tag{4.1}$$

https://doi.org/10.1017/S095679250400539X Published online by Cambridge University Press

The appropriate scalings in the two cases are found to be $\delta_{\mathrm{I}} = \gamma^{2/7}$, $\delta_{\mathrm{II}} = \gamma^{1/5}$. The outer and inner versions of (1.1) are

$$\frac{\partial^2 w}{\partial \tilde{z}^2} = \frac{1}{2}\frac{\partial h}{\partial T} - \frac{\dot{z}_*}{2}\frac{\partial h}{\partial \tilde{z}} + i\gamma \frac{\partial^3}{\partial \tilde{z}^3}\left(\frac{1}{\sqrt{h(\tilde{z})}}\right), \tag{4.2}$$

$$\frac{\partial^2 W}{\partial Z^2} = \frac{\delta}{2}\frac{\partial H}{\partial T} - \frac{\dot{z}_*}{2}\frac{\partial H}{\partial Z} + i \frac{\partial^3}{\partial Z^3}\left(\frac{1}{\sqrt{H(Z)}}\right), \tag{4.3}$$

where

$$w = \begin{cases} \delta_{\mathrm{I}}^2 W & \text{case I} \\ \delta_{\mathrm{II}}^3 W & \text{case II.} \end{cases}$$

We shall restrict attention to similarity solutions, since our ZST solutions fall into this class. Travelling-wave solutions can be treated similarly, but more general, fully-time-dependent, solutions may have very short timescale behaviour when $\gamma \ll 1$, as studied, e.g. by Siegel *et al.* [44, 45]. These authors perform computations at small surface tension $\gamma \ll 1$ in which they choose initial conditions corresponding to a (ZST) Saffman-Taylor finger with $\lambda < 1/2$. The initial evolution indicates that such a finger tries to form, but then, within $O(1)$ time of starting the computation, there is a period of rapid evolution during which events occur on exactly the timescale $\gamma^{2/7}$. This indicates that the corresponding ZST problem has a simple zero in the derivative of the Schwarz function (a case I scenario), but that the inner equation (4.3) in the neighbourhood of the singularity is still fully time-dependent, the term $\delta(\partial H/\partial T)$ appearing at leading order. Our hypothesis is that if initial conditions are such as to force a case I scenario then the solution will rapidly evolve to a case II situation. This is exactly what was observed in the computations of Siegel *et al.* [44, 45]: the period of rapid evolution resulted in a Saffman-Taylor finger with $\lambda = 1/2$, which is a case II scenario.

4.2 Selection for 'similarity solutions'

Boundary points for similarity solutions to the ZST injection problem are of the form $\boldsymbol{r} = (\hat{x}, \hat{y})\sqrt{t}$, where $(\hat{x}, \hat{y})$ lies on the curve $\partial\hat{\Omega} \equiv \partial\Omega(t_0)$ at some time $t = t_0$. The Schwarz function g of $\partial\Omega(t)$ is then defined in terms of $\hat{g}$ (the Schwarz function of $\partial\hat{\Omega}$) by $g(z,t) = \sqrt{t}\hat{g}(\hat{z})$, where $\hat{z} = \hat{x} + i\hat{y}$ is a complex point on $\partial\hat{\Omega}$. Transforming to variables $\hat{z}$, t, the Schwarz function equation (1.1) becomes

$$2\frac{d\hat{w}}{d\hat{z}} = \hat{g}(\hat{z}) - \hat{z}\hat{g}'(\hat{z}) + 2i\hat{\gamma}\frac{d^2}{d\hat{z}^2}\left(\frac{1}{\sqrt{\hat{g}'(\hat{z})}}\right), \tag{4.4}$$

but we have had to redefine $\hat{\gamma} = \gamma/\sqrt{t}$ (with $\hat{\gamma}$ constant), as the non-zero surface tension problem does not permit similarity solutions of this form unless we do. Clearly this is not acceptable in general; however, recall that we are interested in the limit $\gamma \to 0$, which will coincide with the limit $\hat{\gamma} \to 0$. Differentiating again with respect to $\hat{z}$ gives

$$2\frac{d^2\hat{w}}{d\hat{z}^2} = -\hat{z}\hat{h}'(\hat{z}) + 2i\hat{\gamma}\frac{d^3}{d\hat{z}^3}\left(\frac{1}{\sqrt{\hat{h}(\hat{z})}}\right). \tag{4.5}$$

https://doi.org/10.1017/S095679250400539X Published online by Cambridge University Press

Consider again the neighbourhood of a simple or repeated zero of $\hat{h}$ at $\hat{z}=\hat{z}_*$, a fixed point that does not lie at the origin (since the similarity ansatz supposes this to be the injection point). In terms of $\tilde{z}=\hat{z}-\hat{z}_*$ we have

$$2\frac{d^2\hat{w}}{d\tilde{z}^2} = -(\tilde{z}+\hat{z}_*)\hat{h}'(\tilde{z}) + 2i\hat{\gamma}\frac{d^3}{d\tilde{z}^3}\left(\frac{1}{\sqrt{\hat{h}(\tilde{z})}}\right), \tag{4.6}$$

where $\hat{h}\sim O(\tilde{z})$ as $\tilde{z}\to 0$ in case I, and $\hat{h}\sim O(\tilde{z}^2)$ as $\tilde{z}\to 0$ in case II. We find the same inner scalings as before:

$$\begin{aligned} &\text{Case I:} \quad \tilde{z}=\delta Z, \quad \hat{w}=\delta^2 W, \quad \hat{h}=\delta H, \quad \delta=\hat{\gamma}^{2/7},\\ &\text{Case II:} \quad \tilde{z}=\delta Z, \quad \hat{w}=\delta^3 W, \quad \hat{h}=\delta^2 H, \quad \delta=\hat{\gamma}^{1/5}, \end{aligned}$$

giving in both cases the inner equation

$$2\frac{d^2W}{dZ^2} = -(\hat{z}_*+\delta Z)\frac{dH}{dZ} + 2i\frac{d^3}{dZ^3}\left(\frac{1}{\sqrt{H}}\right). \tag{4.7}$$

One may seek solutions to (4.6) and (4.7) as asymptotic expansions

$$\hat{h}\sim\sum_{k=0}^{\infty}\hat{\gamma}^k h_k, \quad H\sim\sum_{k=0}^{\infty}\delta_{\mathrm{I}}^k H_k \text{ (case I)}, \quad H\sim\sum_{k=0}^{\infty}\delta_{\mathrm{II}}^k H_k, \text{ (case II)}. \tag{4.8}$$

Analysis of the equations reveals the form of the asymptotic expansions in each case to be such that:

$$\text{case I:} \quad \begin{aligned} h_k &\sim \tilde{z}\sum_{n=0}^{\infty} c_n^{(k)}\tilde{z}^{n-7k/2} \quad \text{as } \tilde{z}\to 0\\ H_k &\sim Z\sum_{n=0}^{\infty}\mu_n^{(k)}Z^{k-7n/2} \quad \text{as } Z\to\infty; \end{aligned} \tag{4.9}$$

$$\text{case II:} \quad \begin{aligned} h_k &\sim \tilde{z}^2\sum_{n=0}^{\infty} c_n^{(k)}\tilde{z}^{n-5k} \quad \text{as } \tilde{z}\to 0\\ H_k &\sim Z^2\sum_{n=0}^{\infty}\mu_n^{(k)}Z^{k-5n} \quad \text{as } Z\to\infty, \end{aligned} \tag{4.10}$$

with matching between inner and outer regions using the matching principle [49] in the relations

$$\sum_{k=0}^{\infty}\gamma^k h_k \sim \delta_{\mathrm{I}}\sum_{k=0}^{\infty}\delta_{\mathrm{I}}^k H_k, \qquad \sum_{k=0}^{\infty}\gamma^k h_k \sim \delta_{\mathrm{II}}^2\sum_{k=0}^{\infty}\delta_{\mathrm{II}}^k H_k.$$

Thus, while in principle case I appears to be admissible so far, it is clear that construction of such a solution would involve branch point singularities and very delicate matching, and would likely prove impossible. In case II on the other hand the matching can proceed smoothly.

https://doi.org/10.1017/S095679250400539X Published online by Cambridge University Press

The above is related to the work of Combescot *et al.* [12] on the classical Saffman–Taylor problem. The leading-order inner problem is (after one integration)

$$\frac{d^2}{dZ^2}\left(\frac{1}{\sqrt{H_0}}\right)+\frac{i\hat{z}_*}{2}H_0=-i\left(\frac{dW_0}{dZ}+a_0\right), \tag{4.11}$$

with asymptotic behaviour $H_0=O(Z)$ (case I), $H_0=O(Z^2)$ (case II), as $|Z|\to\infty$, or, in terms of $F=1/\sqrt{H_0}$, and $Z=\zeta\sqrt{-2i/\hat{z}_*}$

$$\frac{d^2F}{d\zeta^2}+\frac{1}{F^2}=-\frac{2}{\hat{z}_*}\left(\left(\frac{-\hat{z}_*}{2i}\right)^{1/2}\frac{dW_0}{d\zeta}+a_0\right), \tag{4.12}$$

with asymptotic behaviour $F\sim\lambda_{\rm I}/\sqrt{\zeta}$ (case I), $F\sim\lambda_{\rm II}/\zeta$ (case II), as $|\zeta|\to\infty$, for some complex constants $\lambda_{\rm I}$, $\lambda_{\rm II}$. In Combescot & Ben Amar [12], more or less this same equation (4.12) is derived from the McLean–Saffman formulation [32], but with the right-hand side identically equal to ζ (which up to a multiplicative constant is its leading order behaviour as $|\zeta|\to\infty$ in case I). In Combescot & Ben Amar [12] the authors claim to show that there is no solution of equation (4.12), with right-hand side ζ, that satisfies $F\sim 1/\sqrt{\zeta}$ uniformly at infinity. They do this by setting $F=1/\sqrt{\zeta}+f$ and solving a linearised equation for f, where f is required to decay much faster than $1/\sqrt{\zeta}$ *uniformly* at infinity. If they proved this result then our selection criterion would follow almost immediately, as it would prove the impossibility of a case I similarity solution in the limit $\gamma\to 0$. Unfortunately however their argument is not rigorous, and would require the theory of Stokes lines in asymptotics beyond all orders to make it so (which would be the work of another lengthy paper). Combescot & Ben Amar [12] write down the linearised problem for f as an equation to be solved:

$$\frac{d^2f}{d\zeta^2}-2\zeta^{3/2}f=-\frac{3}{4}\zeta^{-5/2},$$

whose solutions are given in terms of Bessel functions, and cannot be made to decay uniformly as desired at infinity. But in reality the above equation should be an asymptotic relation, with a '$\sim$' replacing the '=' sign, and on the face of it it is possible to construct a naive case I solution of (4.12) that has asymptotic behaviour

$$F\sim\zeta^{-1/2}\sum_{n=0}^{N}\beta_n\zeta^{-7n/2}\quad\text{as }|\zeta|\to\infty,$$

for any finite N. The analogous asymptotic behaviour of a case II solution is:

$$F\sim\zeta^{-1}\sum_{n=0}^{N}\beta_n\zeta^{-5n}\quad\text{as }|\zeta|\to\infty.$$

Nonetheless, in line with our earlier remarks and with the work of Combescot & Ben Amar [12], we claim that there is no acceptable 'case I' type solution to (4.12), and that case II is the only viable option. This claim forms the basis of our selection hypothesis: *In the selected ZST solution, any zeros of the derivative of the Schwarz function must be repeated.*

https://doi.org/10.1017/S095679250400539X Published online by Cambridge University Press

4.3 Other regularisations

We have focussed in the above discussion on the most widely adopted regularisation, namely surface tension. However, it is clear that our proposed selection criterion is independent of the regularisation adopted and, just as in the Saffman-Taylor problem $\lambda = 1/2$ is selected by many distinct regularisations, we believe the same will be true in the present case. More specifically, for the kinetic undercooling regularisation it has recently been shown [10] that $\lambda = 1/2$ is selected in the limit of zero kinetic undercooling, and the beyond-all-orders selection mechanism is related to the coincidence of the singularities that occurs in this special case; similar arguments pertain for other regularisations also. It should be noted, however, that some regularisations of Saffman–Taylor do not select $\lambda = 1/2$ [4, 5, 46]; $\lambda \to 0$ or $\lambda \to 1$ is typically selected when the appropriate limits are taken in these cases, and the analogous solutions from our ZST solution family could be conjectured to apply here also. The conformal map (3.23) representing our solutions simplifies considerably in these two special cases. The angular finger width is given by $\lambda = 1 - N/\mu$, so writing $1/\mu = 1/N - \epsilon_1$ for some small positive parameter ϵ_1, and rescaling time $t = \epsilon, \tau$ (since a vanishingly thin finger moves with infinite speed) the $\lambda \to 0$ ZST solution is given by the mapping function

$$Z(\zeta) = \Lambda_0 e^{i\pi/N} \zeta^{-1/N} + O(\epsilon_1), \quad \Lambda_0 = \sqrt{\frac{Q\tau \Gamma\left(\frac{2}{N} + \frac{1}{2}\right)}{\sqrt{\pi}\Gamma\left(\frac{2}{N}\right)}}.$$

In the limit $\lambda \to 1$ we write $1/\mu = \epsilon_2 \ll 1$ and recover the mapping function

$$Z(\zeta) = \frac{\sqrt{2Qt}}{2}\left\{\left[(1-\zeta)^{1/2} + i\sqrt{\zeta}\right]^{2/N} + \left[(1-\zeta)^{1/2} - i\sqrt{\zeta}\right]^{2/N} + 2i \sin\left(\frac{2}{N}\sin^{-1}\sqrt{\zeta}\right)\right\} + O(\epsilon_2).$$

In each case one-half of the free boundary is given by the image of the real interval $\zeta \in [0, 1]$, giving a moving semi-infinite slit in the case $\lambda \to 0$, and an arc of a circle in the case $\lambda \to 1$.

Both these limits have 'special' singularity structure in the complex plane. For $\lambda \to 0$ we find that the leading-order Schwarz function satisfies

$$G'(\zeta) = -\frac{1}{N}\Lambda_0 e^{-i\pi/N}\zeta^{-1/N-1}, \qquad G''(\zeta) = \frac{1}{N}\left(\frac{1}{N} + 1\right)\Lambda_0 e^{-i\pi/N}\zeta^{-1/N-2},$$

so $G'(\zeta)$ and $G''(\zeta)$ vanish as $|\zeta| = \infty$, and there are no zeros in the finite ζ-plane. For $\lambda \to 1$ we find that that $G'(\zeta)$ has a zero only where

$$\exp(-2iu/N) = 0, \quad u = \sin^{-1}\sqrt{\zeta},$$

and that this is exactly the condition for $G''(\zeta)$ to vanish also. Hence there is a repeated zero of $G'(\zeta)$ at $\zeta = -\infty$ (real and negative), and in fact this is the only root of $G'(\zeta)$.

https://doi.org/10.1017/S095679250400539X Published online by Cambridge University Press

5 Selection of the wedge angle

We now apply the selection criterion put forward in § 4.2 to our family of ZST wedge solutions.

The Schwarz function is related to the Baiocchi transform variable u via

$$g(z,t) = \bar{z} - 2(u_x - iu_y),$$

because the boundary conditions (3.4) on u imply that both u_x and u_y vanish on $\Gamma(t)$ (so the Schwarz function identity holds on $\Gamma(t)$), and in addition the real and imaginary parts of $g(z,t)$ thus defined have continuous partial derivatives in some neighbourhood of $\Gamma(t)$ which satisfy the Cauchy-Riemann equations. Thus g is complex analytic in a neighbourhood of $\Gamma(t)$, and by uniqueness, must be the Schwarz function of $\Gamma(t)$. In terms of the function $W(z)$ introduced in (3.9) then, $-g^-(z) = z + 2W(z)$, where we use a '$-$' superscript to denote the fact that this is the Schwarz function only of $\Gamma^-(t)$. In terms of ζ, writing $G^-(\zeta) = g^-(\mathscr{Z}(\zeta))$,

$$G^-(\zeta) = -(\mathscr{Z}(\zeta) + 2\mathscr{W}(\zeta)). \tag{5.1}$$

However, we do not need to evaluate $\mathscr{W}(\zeta)$ explicitly to find G^- if we observe that on the boundary $\Gamma^-(t)$,

$$\bar{z} = \overline{\mathscr{Z}(\zeta)} = \overline{\mathscr{Z}(\bar{\zeta})} = \bar{\mathscr{Z}}(\zeta)$$

(the last equality defines the complex conjugate function $\bar{\mathscr{Z}}(\zeta)$), the middle equality holding because $\zeta \in \mathbb{R}$ on the free boundary. Thus by analytic continuation away from Γ^- we obtain $G^-(\zeta) = \bar{\mathscr{Z}}(\zeta)$ on the upper half ζ-plane. Analogous to (3.25) we can write down the combined Schwarz function $G(\zeta)$ for the composite (analytic) curve $\Gamma(t) = \Gamma^-(t) \cup \Gamma^+(t)$:

$$G(\zeta) = \begin{cases} \bar{\mathscr{Z}}(\zeta) & \Im(\zeta) > 0, \\ e^{-2\pi i/N}\mathscr{Z}(\zeta) & \Im(\zeta) < 0; \end{cases} \tag{5.2}$$

again this defines a function analytic on the ζ-plane slit along $[0,1]$. Since the Schwarz function for the whole curve satisfies $G(\zeta) \equiv g(\Sigma(\zeta))$, and $\Sigma(\zeta)$ is a conformal map, it is easily seen that a repeated zero of g' must correspond to a repeated zero of G'. Also, $G(\zeta)$ must satisfy the generalised hypergeometric equation (3.16), since $\mathscr{Z}(\zeta)$ (and hence $\bar{\mathscr{Z}}(\zeta)$, since the coefficients of (3.16) are real) does. It is clear from (3.16) then that at a point where $G'(\zeta_*) = 0 = G''(\zeta_*)$, we require either $G(\zeta_*) = 0$ also, or

$$\zeta_* = \frac{N^2}{\mu_*}\left(\frac{1}{2} + \frac{1}{\mu_*}\right). \tag{5.3}$$

Equation (5.3) provides one relation between the critical value μ_* and the location ζ_* (which must be real) of the repeated zero of $G'(\zeta)$, but we have been unable to find another explicit relation to fix the parameters uniquely. Hence for a given value of N our approach is to vary the value of the parameter μ, find the corresponding complex zero(s) of $G'(\zeta)$ in the upper half ζ-plane (there will be another complex conjugate zero in the lower half-plane), and determine for which value of μ the zero-pair coalesces on the

https://doi.org/10.1017/S095679250400539X Published online by Cambridge University Press

real axis. The explicit expression for $G(\zeta)$ is found from the solution for $\mathscr{Z}(\zeta)$. It is not possible to determine the zeros of G' in the upper half ζ-plane analytically, so we search for them numerically, using Maple. The results of this search are shown in figure 8 for the cases $N=1$, 2, 3. For $N=1$ we have $\mu_* \approx 1.09473$ and $\zeta_* \approx 1.2911$; for $N=2$ $\mu_* \approx 2.34966$, $\zeta_* \approx 1.5757$; for $N=3$ $\mu_* \approx 3.72692$, $\zeta_* \approx 1.8553$. It may be verified that these approximate values ζ_* and μ_* satisfy (5.3). The size of the wedge angle in the air in a given solution is $\beta \equiv 2\pi(1/N - 1/\mu)$ radians. The solutions for the critical wedge angles are shown in Figures 4, 5 and 6, for several different values of $(t_w - t)$.

6 Selection for the case $N=4$

As observed by other authors ([3] for the convergent geometry considered here, and Ben Amar [2] and Brener *et al.* [6] for the divergent geometry), when there is four-fold symmetry, the solutions simplify considerably. The zeros of $G'(\zeta)$ that are responsible for selection lie in $|\zeta|>1$, and the relevant form of the map in this case is (3.22), which, after setting $N=4$ and simplifying, leads (by (5.2)), to the following expression for the Schwarz function $G(\zeta)$ in $\Im(\zeta)>0$, $|\zeta|>1$:

$$G(\zeta) = \left(\frac{Qt}{\left(1+\frac{4}{\mu}\right)\cos\frac{2\pi}{\mu}}\right)^{1/2} 2e^{-i\pi/4}\zeta^{1/4}\sin\left(\left(\frac{1}{2}+\frac{2}{\mu}\right)\sin^{-1}\frac{1}{\sqrt{\zeta}}\right). \tag{6.1}$$

We already have one condition, (5.3), that must hold at a repeated zero of $G'(\zeta)$:

$$\zeta_* = \frac{8}{\mu_*^2}(\mu_*+2). \tag{6.2}$$

Differentiating (6.1) and setting the result to zero provides a second condition,

$$\cos^2\left(\left(\frac{1}{2}+\frac{2}{\mu_*}\right)\sin^{-1}\frac{1}{\sqrt{\zeta_*}}\right) = \frac{\zeta_*-1}{\left(1+\frac{4}{\mu}\right)^2+\zeta_*-1}. \tag{6.3}$$

Eliminating ζ_* between (6.2) and (6.3) gives a single algebraic equation for μ_*,

$$\cos^2\left(\left(\frac{1}{2}+\frac{2}{\mu_*}\right)\sin^{-1}\frac{\mu_*}{\sqrt{8(\mu_*+2)}}\right) = \frac{-\mu_*^2+8\mu_*+16}{16(\mu_*+2)}. \tag{6.4}$$

In the relevant range (that is, $\mu>4$) this has solution $\mu_* = 5.197700$, providing a direct verification of the value given in Table 1, found by the root-tracking method.

The analogous selection problem for the case of growing air fingers, i.e. the divergent geometry, was considered by Brener *et al.* using a WKB approach.

7 Comparison with numerical results

When comparing our theoretical predictions with the available numerical results, it must be emphasised that one can only talk meaningfully about a 'wedge angle' in the limit $\gamma \to 0$, and not for a fixed value of γ. We believe the numerics of Nie & Tian [8] to be the most careful and accurate, and take comparison with these more seriously than with the numerics of Ceniceros *et al.* [33]. Moreover, in Nie & Tian [8], progressively smaller

https://doi.org/10.1017/S095679250400539X Published online by Cambridge University Press

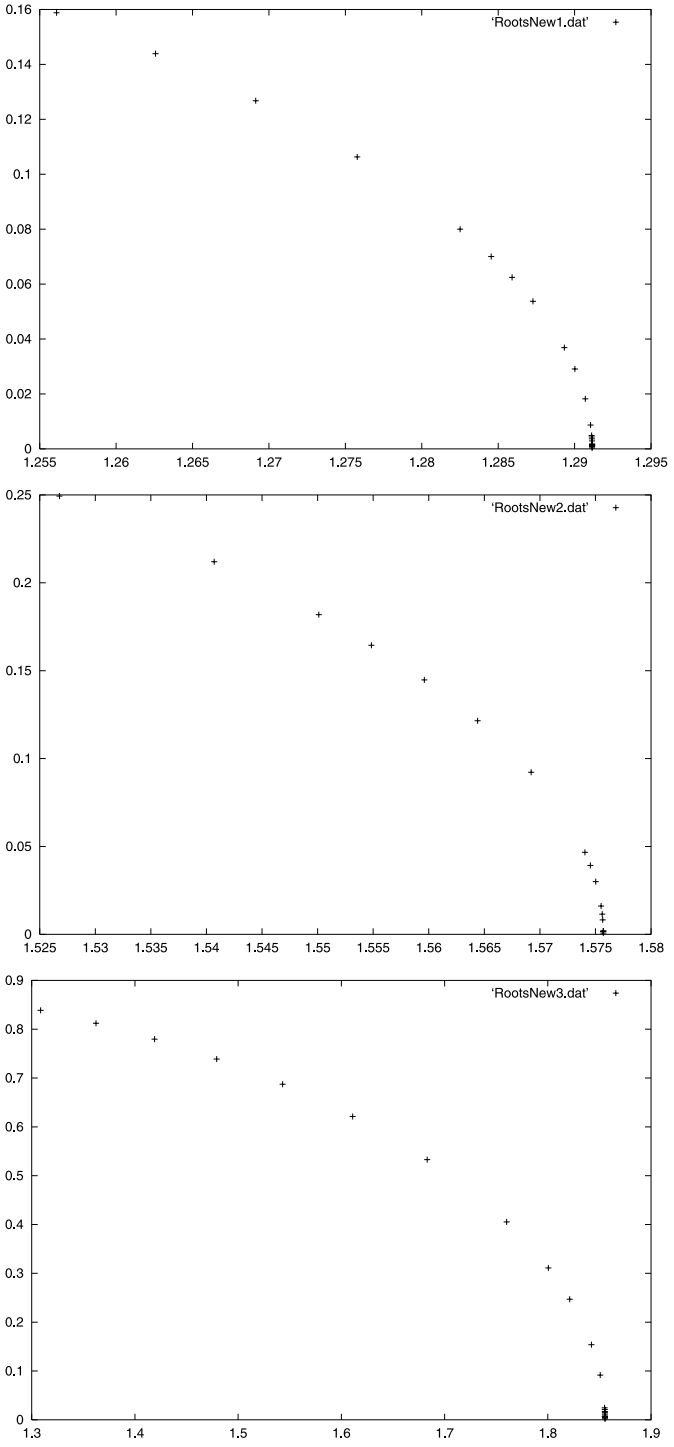

FIGURE 8. Cases $N = 1, 2, 3$: The location of the upper zeros of $G'(\zeta)$ as μ is decreased towards the critical value. The complex conjugate zero is not shown. The movement of the zero onto the real axis at the point $\zeta = \zeta_*$ when $\mu = \mu_*$ is clearly demonstrated. For $\mu > \mu_*$ there is only one simple zero of G', to the right of ζ_*.

https://doi.org/10.1017/S095679250400539X Published online by Cambridge University Press

Table 1. *Table of N versus the selected values of μ, and the corresponding angles of the air wedges formed*

N	μ_*	β_* (radians)	β_* (degrees)
1	1.09473	0.54372	31.15°
2	2.34966	0.46751	26.79°
3	3.72692	0.40850	23.41°
4	5.19770	0.36196	20.74°
5	6.74088	0.32454	18.59°

Table 2. *The values of surface tension versus wedge angle found by Ceniceros* et al. [8] *(Table II)*

j	γ_j	β_j (radians)	β_j (degrees)
1	8×10^{-4}	0.67459	38.65°
2	4×10^{-4}	0.65719	37.65°
3	2×10^{-4}	0.64399	36.89°
4	1×10^{-4}	0.63660	36.47°
5	5×10^{-5}	0.63359	36.30°

values of γ are taken (and these values are orders of magnitude smaller than those used by Ceniceros *et al.* [33]), so that their numerics give more credence to the idea of a limiting angle. Comparison cannot be made with the numerics of Kelly & Hinch [28].

The case $N = 1$

For the case $N = 1$ Ceniceros *et al.* tabulated values for the wedge angle $\beta_j \equiv 2\pi(1 - 1/\mu_j)$ (that is, the total angle in the air, not the fluid) for several different values γ_j of the surface tension coefficient. Their results are displayed in Table 2. Our results give a critical value $\beta_* \equiv 2\pi(1-1/\mu_*) = 0.54372$ radians (31.15°), showing a discrepancy of about 0.08987 radians (5.15°) with their final value calculated, our wedge of air being narrower than theirs. However, as is clear from their figures (see Figures 1 and 11 reproduced from Ceniceros *et al.* [8]) the free boundary in their calculations is only locally a wedge: away from the tip the global geometry influences the free boundary, making it more of a spindle shape. The tangent angle changes continuously between 'inner' and 'outer' regions, and it is difficult, if not impossible, to give a definitive 'wedge angle'. (The authors give no details of how they arrived at their tabulated values.) In fact, simply drawing tangents on figure 11 and using a protractor to measure the wedge angle appears to give a value of around 32° for β_5, so we are not discouraged by this apparent numerical discrepancy.

A more useful comparison, we feel, is provided by plots of the tangent angle to the free boundary versus a scaled arclength variable, α. Ceniceros *et al.* give such plots for three different times approaching the blow-up, i.e. wedge-formation, time (Figure 4 in Ceniceros *et al.* [8]; reproduced in Figures 9 and 10 here). This they do for surface

https://doi.org/10.1017/S095679250400539X Published online by Cambridge University Press

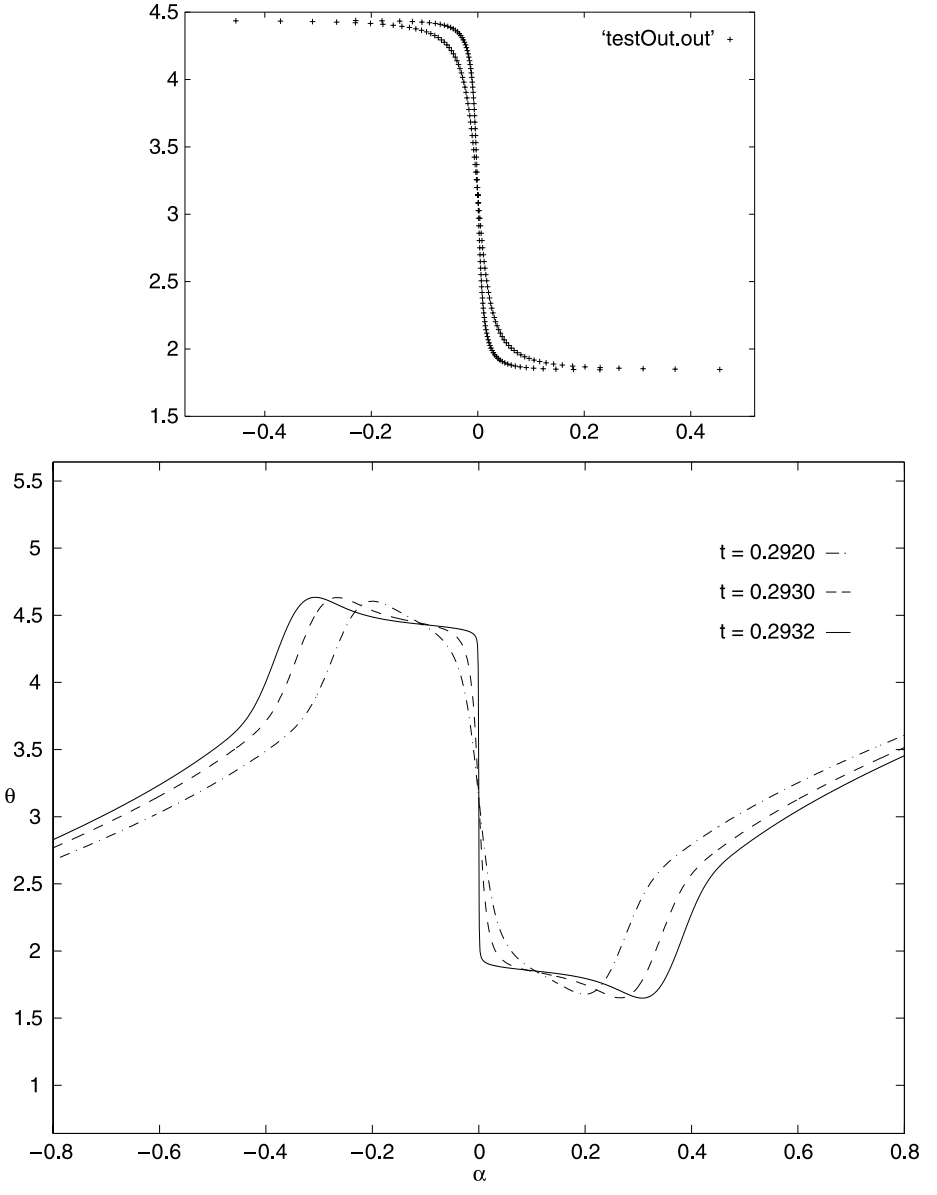

FIGURE 9. The tangent angle θ to $\Gamma(t)$, as a function of scaled arclength α along $\Gamma(t)$, for times approaching solution breakdown. The upper plot is ours, obtained for the critical angle solution $\mu_* = 1.09473$ ($\beta_* = 0.54372$), and is shown at times $t = 0.0002$, $t = 0.0012$. The lower plot is that obtained numerically by Ceniceros *et al.* (Figure 4 in Ceniceros *et al.* [8]), for dimensionless surface tension $\gamma_2 = 4 \times 10^{-4}$ (reproduced by kind permission of the authors).

tension $\gamma_2 = 4 \times 10^{-4}$, for which they give the final wedge angle as $\beta_2 = 0.65719$. We give analogous plots for our exact ZST solution, both for their estimated wedge angle $\beta_2 = 0.65719$ (Figure 10), and for the critical wedge angle $\beta_* \equiv 2\pi(1 - 1/\mu_*) = 0.54372$ that we found above (Figure 9).

https://doi.org/10.1017/S095679250400539X Published online by Cambridge University Press

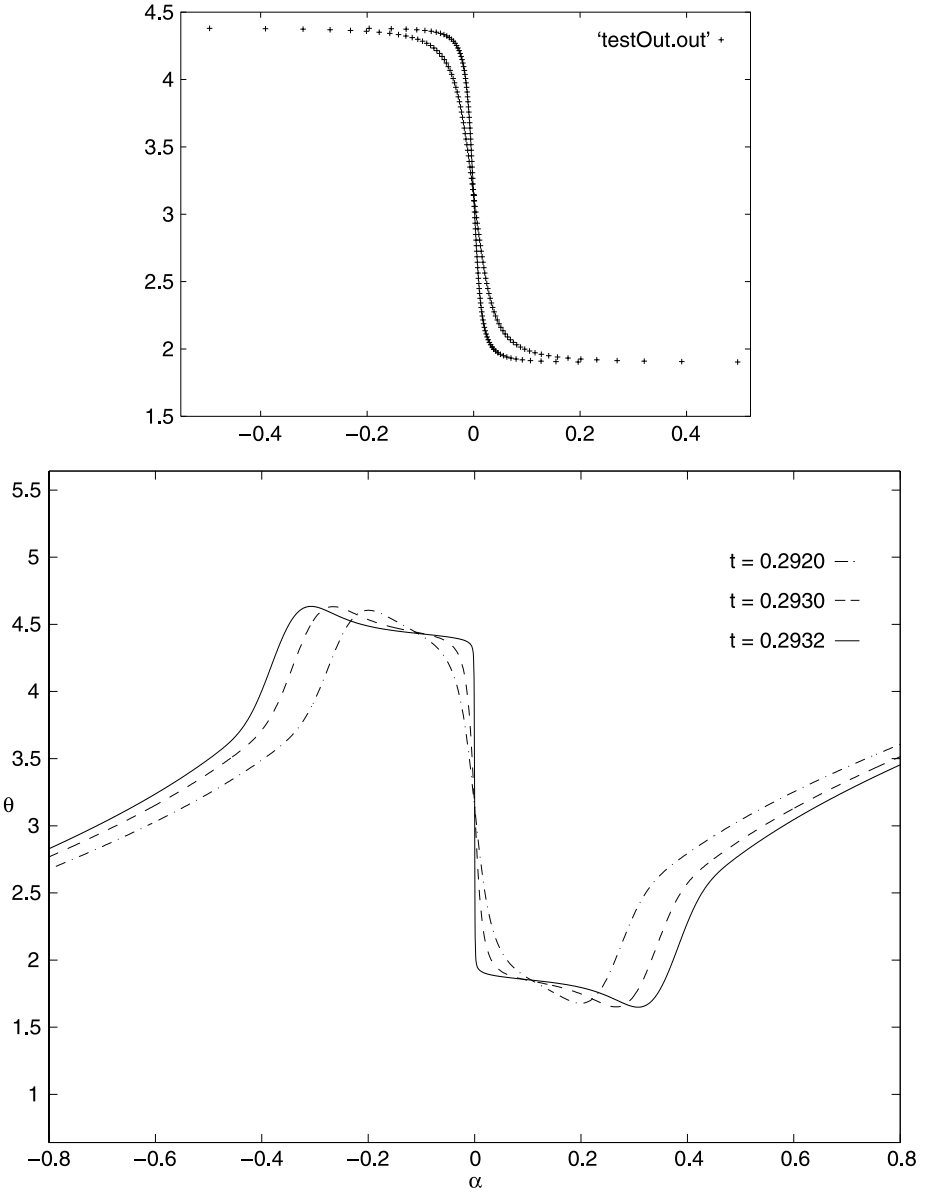

FIGURE 10. The tangent angle θ to $\Gamma(t)$, as a function of the scaled arclength α along $\Gamma(t)$, for times approaching solution breakdown. The lower plot is that obtained numerically by Ceniceros *et al.* (Figure 4 in Ceniceros *et al.* [8]), for dimensionless surface tension $\gamma_2 = 4 \times 10^{-4}$ (reproduced by kind permission of the authors). The upper plot is ours, obtained for the solution with $\beta_2 = 2\pi(1 - 1/\mu_2) = 0.65710$ (the wedge angle estimated in Ceniceros *et al.* [8] for this value of γ), and shown at times $t = 0.0002$, $t = 0.0012$.

There were certain estimates that had to be made in producing these figures. Firstly, to calculate the corresponding times at which to plot our ZST solution, we assumed that $t = 0.2932$ in the numerical results, which is the latest time for which Ceniceros *et al.*

https://doi.org/10.1017/S095679250400539X Published online by Cambridge University Press

were able to calculate accurately, corresponded to blow-up time t_w. We thus plotted our injection solution at times $t = (0.2932 - 0.2930) = 0.0002$ and $t = (0.2932 - 0.2920) = 0.0012$, corresponding to the dashed and dash-dotted curves of Ceniceros *et al.*, respectively. Secondly, the arclength variable α used by Ceniceros *et al.* is scaled so that it always increases from 0 to 2π along the interface. Since the interface changes length at each timestep, we had to estimate (carefully) the length of the interface for the solution of Ceniceros *et al.* [8] at times $t = 0.2920$ and $t = 0.2930$, from the corresponding free boundary plots given in Figure 3 of Ceniceros *et al.* [8]. (Our estimates were 4.41 and 4.55 length units, respectively.) Once this was done we were able to calculate the correct scaling factor to convert arclength to α at these times, and plot our results for tangent angle against this scaled arclength for a direct comparison. The theoretical and numerical results are displayed on same-scale axes.

Overlaying the plots, the agreement between theory and numerics in Figure 9, which shows our ZST solution for our critical wedge angle β_*, is remarkably good in the crucial region around the wedge tip ($\alpha = 0$). The theoretical curves follow closely the dashed and dash-dotted numerical curves, and the abrupt change in tangent angle appears to fit almost exactly. The fit for Figure 10, which shows our ZST solution for the wedge angle $\beta_2 = 0.65719$ (estimated by Ceniceros *et al.* [8]), is less good, the abrupt change in tangent angle in our theoretical plot being too small.

Figures 9 and 10 may also be compared with Figure 6 in Nie & Tian [33].[4] At first sight, agreement with these results is markedly less good; from their plots of tangent angle versus arclength along the boundary, we estimate their wedge angle β as breakdown is approached to be about 0.76 radians (43.5°). However, the smallest value of the dimensionless surface tension they compute with is 0.002, which is an order of magnitude larger than any value considered by Ceniceros *et al.* [8], and the results there clearly indicate β increasing with surface tension. When the wedge angles β_j tabulated in Ceniceros *et al.* [8] (and reproduced in Table 2) are plotted against the surface tension values γ_j, if the values for $j = 1$ are neglected (the largest value of surface tension) the points lie on a line. Extrapolating this linear relation to the larger surface tension value $\gamma = 0.002$ used by Nie & Tian gives an estimate of $\beta = 0.766$ for the expected wedge angle. (That this is a little larger than 0.76 is in line with our observations above, that we believe the wedge angles given in Table 2 to be overestimates of the 'true' angles.) So there is better agreement than was originally apparent between the numerics of Nie & Tian [33] and Ceniceros *et al.* [8], and hence better agreement than at first appears between our results and those of Nie & Tian [33].

Another check on our results is provided by considering the magnitude of the curvature at the developing wedge-tip. Plots of interface curvature against scaled arclength α are given in figure 6 of [8] for surface tension $\gamma_5 = 5 \times 10^{-5}$, at times $t =$ 0.2860, 0.2880, 0.2916, 0.29181. Clearly, for our solution this varies like $1/\sqrt{t_w - t}$, time $t = t_w$ corresponding to the wedge configuration. So, if κ_{tip} is the curvature at the wedge-tip then we have

$$|\kappa_{\text{tip}}| = \frac{K_\mu}{\sqrt{t_w - t}},$$

[4] The numerics of Kelly & Hinch [28] are not taken sufficiently near to wedge formation time to be able to make a comparison with our theory.

https://doi.org/10.1017/S095679250400539X Published online by Cambridge University Press

where the constant of proportionality K_μ depends only upon the wedge angle (and hence only on the parameter μ). For our critical value μ_* we find $K_{\mu_*} = 2.251$, while for the critical angle estimated by Ceniceros *et al.* for this value of surface tension ($\beta_5 = 2\pi(1 - 1/\mu_5) = 0.63359$) we find $K_{\mu_5} = 1.633$.

For such small surface tension, the numerical interface evolution in Ceniceros *et al.* [8] must be almost exactly that of a ZST solution, and hence the curvature at the wedge tip should again behave like $1/\sqrt{t_w - t}$:

$$\kappa_{\text{tip}} = \frac{K}{\sqrt{t_w - t}}.$$

For the times $t = 0.2916$, 0.29181 the tip curvatures given in Ceniceros *et al.* [8] are $\kappa_{\text{tip}} = -133.3$, -1371.1 respectively, from which the blow-up time t_w may be estimated using

$$K = -133.3\sqrt{t_w - 0.2916} = -1371.1\sqrt{t_w - 0.29181}.$$

This gives $t_w = 0.291812$, showing that blow-up had almost been reached by the final calculation, as we expect. Using this estimate for t_w, we can calculate values for the constant of proportionality K for times $t_1 = 0.2860$, $t_2 = 0.2880$, $t_3 = 0.2916$, $t_4 = 0.29181$, using the curvature values given in [8]. In principle these values should be the same, if the behaviour is self-similar. We find:

$$K_1 = 3.049, \quad K_2 = 2.568, \quad K_3 = 1.941, \quad K_4 = 1.941.$$

indicating that the first two calculations are too early for the behaviour to be truly self-similar.[5] Obviously K_3 and K_4 are equal, given the manner of calculating t_w, and probably provide the most reliable estimate, being in the self-similar regime. This value of K lies almost exactly mid-way between the values K_{μ_*} (for our critical angle) and K_{μ_5} (for the critical angle estimated by Ceniceros *et al.*) given above for the idealised ZST solution. Thus from the curvature measurements alone, it is hard to say which value (μ_* or μ_5) is the closest to that observed numerically.

The case $N = 2$

There are several calculations in Nie & Tian [33] that show more than one wedge going into the sink, but only one of these has the rotational symmetry assumed here. This is a calculation with two air wedges going into the sink, and is illustrated in Figure 14 of Nie & Tian [33]. The authors do not give an estimate of the wedge angle, nor do they plot tangent angle as a function of arclength for this calculation. Using a protractor we were able to make an estimate of the angle of one of the air wedges: $\beta \approx 37^\circ$ (0.645 radians). Our results give the selected wedge angle as $\beta_* = 2\pi(1/N - 1/\mu_*) \approx 0.4674$ radians (26.78°; see Figure 5 for a plot of the evolution of this solution). In the case $N = 1$ the ratio of the two β-values: (Nie & Tian)/(ours) is about 1.39, and in the case $N = 2$ this ratio is about 1.38. Given our earlier argument showing that the agreement between our results and

[5] Taking the average of all four values gives a value $K = 2.375$, much closer to K_{μ_*} than to K_{μ_5}, but this is perhaps a little hopeful.

https://doi.org/10.1017/S095679250400539X Published online by Cambridge University Press

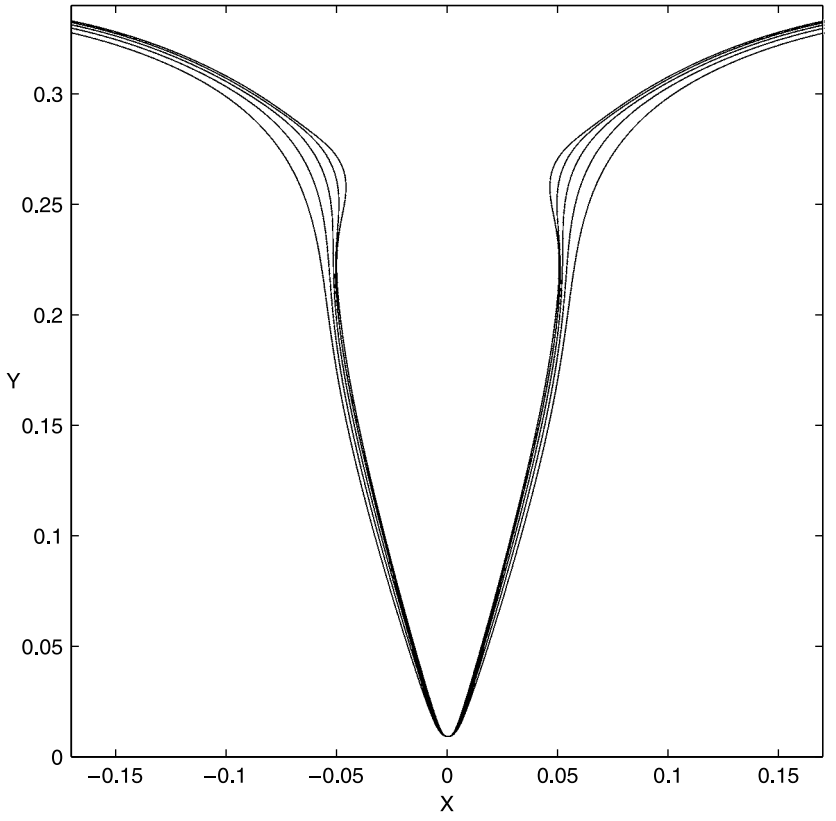

FIGURE 11. The wedge-like configurations obtained in Ceniceros *et al.* [8] for a sequence of surface tension values: 8×10^{-4}, 4×10^{-4}, 2×10^{-4}, 1×10^{-4}, and 5×10^{-5} (the wedge angle β decreases with the surface tension). This plot may be compared with our solution of Figure 4. Reproduced by kind permission of the authors.

theirs in the $N = 1$ case is better than was at first apparent (the wedge angle β decreasing markedly with surface tension according to the results of Ceniceros *et al.* [8]), the same applies here.

Other values of N

Ben Amar [3] has carried out the numerical solution for self-similar flow in a wedge-shaped Hele–Shaw cell at small surface tension, in the case that air wedges approach the apex of the cell as fluid is removed there. (A time-dependent suction rate is imposed to ensure the existence of a self-similar solution.) This is analogous to our problem if the angle between the cell walls, $|\theta_0|$ in the notation of Ben Amar [3], can be identified with our angle of rotational symmetry $2\pi/N$.

In Figure 3 of Ben Amar [3] the author plots the selected angular width λ as a function of the surface tension parameter for $|\theta_0| = 20°$, corresponding to $N = 18$ in our solutions. The lowest value of surface tension calculated for, $\sigma = 0.00025$, gives a value $\lambda = 0.43$;

https://doi.org/10.1017/S095679250400539X Published online by Cambridge University Press

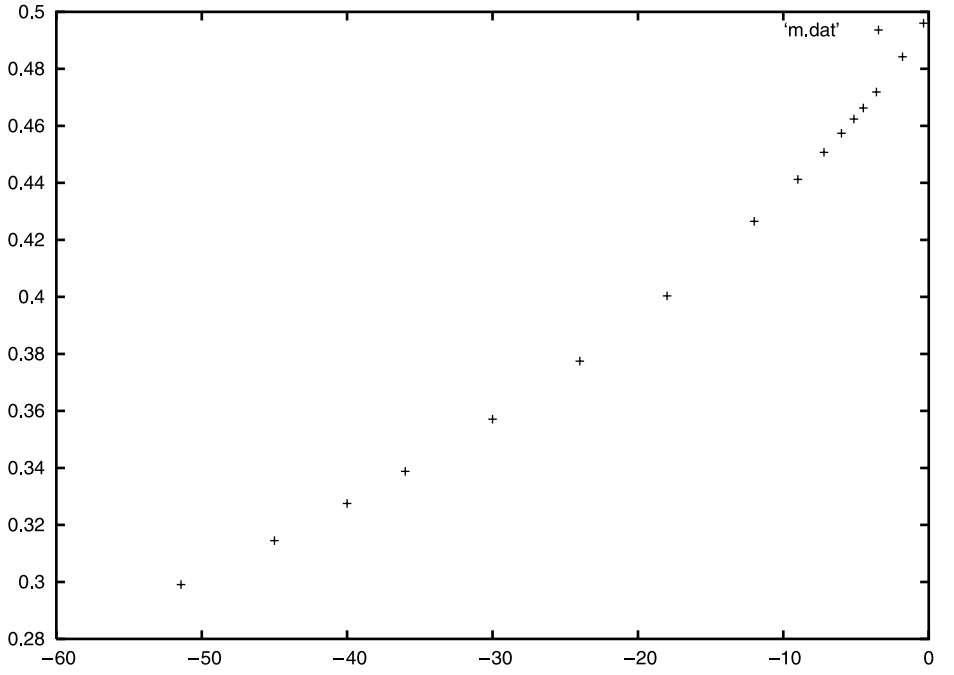

FIGURE 12. Plot of the selected value λ_* versus the angle $-(360/N)$, computed for various values of N between 7 and 1000. This represents the $\gamma = 0^+$ limit of figure 4(b) in Ben Amar [3].

extrapolation of the numerical results to $\sigma = 0$ appears to give a value of $\lambda \approx 0.41$. Using our selection criterion on our $N = 18$ ZST solution gives a value $\lambda_* = 0.3924$.

In Figure 4(b) of Ben Amar [3] the author plots the quantity λ (the fraction of the Hele–Shaw cell that is occupied by the air wedge as it approaches the origin) as a function of the cell angle (in degrees) θ_0 for four different fixed values of γ, the smallest being 0.0004. The conventions adopted in Ben Amar [3] mean that negative values of θ_0 correspond to converging-wedge solutions, so only the region $\theta_0 < 0$ is relevant for comparison with our results.

In Figure 12 we give the analogous plot in the limit $\gamma \to 0$, of $\lambda_* \equiv 1 - N/\mu_*$ versus $-(360/N)$. We have compared Figure 12 here to Figure 4(b) of Ben Amar [3] on same-scale axes, and our results look very plausible as the ZST limit of the curves given in Ben Amar [3]. Our curve is still some way from the $\gamma = 0.0004$ curve of Ben Amar [3], but as we have already seen from the numerics of [8] versus those of Nie & Tian [33], surface tension has to be taken very small indeed before the ZST behaviour is approximated.

The convergence of λ_* to the value $1/2$ as $N \to \infty$ is clearly indicated. We now consider this limit analytically.

8 The limit $N \to \infty$

In the limit as the parameter $N \to \infty$ we can derive the selection criterion asymptotically. In this case the sector angle $2\pi/N$ gets narrower and narrower: the geometry approaches

https://doi.org/10.1017/S095679250400539X Published online by Cambridge University Press

that of the classical Saffman–Taylor problem, and hence the (selected) ratio $\lambda_* := 1-N/\mu_*$ (the fraction of the fundamental fluid wedge occupied by the air) should approach the value $1/2$ as $N \to \infty$.

From Figure 2 we can see that $(1/\mu) < (1/N)$. Writing $N = 1/\epsilon$ $(0 < \epsilon \ll 1)$ we make the ansatz

$$\frac{1}{\mu_*} = a_0\delta + o(\delta) \quad \text{as } \delta(\epsilon) \to 0,\ \epsilon \to 0, \tag{8.1}$$

for $0 < a_0 < 1$, and then from the relation (5.3) between μ_* and the location ζ_* of the repeated zero we have

$$\zeta_* = \frac{a_0\delta}{2\epsilon^2} + o(\delta)/\epsilon^2. \tag{8.2}$$

We obtain an explicit expression for the Schwarz function in the ζ-plane, $G(\zeta)$, from (5.2), with $\mathscr{Z}(\zeta)$ given by (3.23):

$$G(\zeta) = \Lambda\left\{\frac{\Gamma\left(\frac{1}{2}+\frac{2}{\mu}\right)e^{-i\pi/\mu}\zeta^{-1/\mu}}{\Gamma\left(\frac{1}{2}+\frac{1}{N}+\frac{1}{\mu}\right)\Gamma\left(1+\frac{1}{N}+\frac{1}{\mu}\right)}F\left(\frac{1}{N}-\frac{1}{\mu},-\frac{1}{N}-\frac{1}{\mu};\frac{1}{2}-\frac{2}{\mu};\zeta\right)\right.$$
$$\left. + i\frac{\Gamma\left(-\frac{1}{2}-\frac{2}{\mu}\right)e^{i\pi/\mu}\zeta^{1/2+1/\mu}}{\Gamma\left(\frac{1}{N}-\frac{1}{\mu}\right)\Gamma\left(\frac{1}{2}+\frac{1}{N}-\frac{1}{\mu}\right)}F\left(\frac{1}{2}+\frac{1}{N}+\frac{1}{\mu},\frac{1}{2}-\frac{1}{N}+\frac{1}{\mu};\frac{3}{2}+\frac{2}{\mu};\zeta\right)\right\} \tag{8.3}$$

(Λ is given by (3.24)). Since we have already imposed the relation (5.3) we only need ensure that $G'(\zeta_*) = 0$ to leading order, to obtain the leading order selection result.

The asymptotic forms of the Gamma functions and powers are easily obtained. Consider the first hypergeometric function, which we denote by $F_1(\zeta)$. Using results from Abramowitz & Stegun [1], we find

$$\frac{dF_1}{d\zeta} = -2\left(\epsilon^2 - \delta^2 a_0^2\right)\frac{\sin^{-1}\sqrt{\zeta}}{\sqrt{\zeta(1-\zeta)}} + o(\epsilon^2, \delta^2)$$

hence by integration

$$F_1(\zeta) = 1 - 2\left(\epsilon^2 - \delta^2 a_0^2\right)((\sin^{-1}\sqrt{\zeta})^2 + k) + +o(\epsilon^2, \delta^2)$$

where k is a constant. For the second hypergeometric function ($F_2(\zeta)$) we have

$$F_2(\zeta) = \frac{\sin^{-1}\sqrt{\zeta}}{\sqrt{\zeta}} + o(1) \qquad \frac{dF_2}{d\zeta} = \frac{1}{2\zeta\sqrt{1-\zeta}} - \frac{\sin^{-1}\sqrt{\zeta}}{2\zeta\sqrt{\zeta}} + o(1).$$

We now have all the information we require to evaluate the leading-order term in $dG/d\zeta$ at the point ζ_*, and set this to zero for the selection condition. When doing this we ignore the term Λ, since this premultiplies everything. We find that a balance of leading-order terms is possible only if $\delta = \epsilon$, and that in this case

$$\frac{G'(\zeta)}{\Lambda} = -2\epsilon^2\left(1 \pm \frac{a_0 - 1}{a_0}\right) + o(\epsilon^2)$$

https://doi.org/10.1017/S095679250400539X Published online by Cambridge University Press

the choice in sign arising from a square-root. This term can be zero only if $a_0 = 1/2$, with the '+' sign. Hence as $N \to \infty$ we have

$$\frac{1}{\mu_*} = \frac{1}{2N} + o(1/N), \quad \zeta_* = \frac{N}{4} + o(N), \tag{8.4}$$

and so the fraction of the fundamental wedge $2\pi/N$ occupied by the air wedge is

$$\lambda_* \equiv 1 - \frac{N}{\mu_*} = \frac{1}{2} + o(1), \quad \text{as } N \to \infty.$$

As we have seen, our numerical results appear to obey (8.4) for large values of N.

Using the above limiting forms of the hypergeometric functions, and the selected value of a_0, it is easy to verify that the asymptotic form of the map is

$$\frac{\mathscr{Z}(\zeta)}{\Lambda} = (\text{real const.}) + \epsilon\left(-\frac{1}{2}\log\zeta + i\sin^{-1}\sqrt{\zeta} + i\frac{\pi}{2}\right) + o(\epsilon).$$

The free boundary is the image of the real ζ-axis between 0 and 1 under this map; hence in suitably scaled coordinates the cartesian equation of the boundary is given by

$$y(x) = \frac{\pi}{2} + \sin^{-1}(e^{-x}), \quad x > 0$$

(different branches of the inverse sine function give the two sides of the free boundary) which is exactly the Saffman–Taylor finger for $\lambda = 1/2$.

9 The NZST problem

In a real problem of this kind, however small the surface tension parameter is, it must ultimately become significant and dominate the free boundary evolution as the wedge-tip forms. In the following we examine the effects of surface tension, which become important only very near the blow-up time.

9.1 The limit $\gamma \to \infty$

However small surface tension is taken in a calculation, in the ultimate stage of the evolution (as the wedge tip forms) it must in fact be the dominant effect. Hence in these ultimate stages it is appropriate to consider the limit of infinite surface tension. Here there are two timescales. The initial transient has

$$t = \gamma^{-1}\hat{t}, \quad p = \gamma^{-1}\hat{p}, \quad v_n = \gamma\hat{v}_n,$$

during which negligible fluid is extracted, so that at leading order we have

$$\begin{gathered} \nabla^2\hat{p}_0 = 0 \quad \text{throughout } D_0(\hat{t}), \\ \hat{p}_0 = \kappa_0, \quad \frac{\partial\hat{p}_0}{\partial n} = -\hat{v}_{0n} \quad \text{on } \partial D_0(\hat{t}). \end{gathered} \tag{9.1}$$

https://doi.org/10.1017/S095679250400539X Published online by Cambridge University Press

Since

$$\int\int_{D_0(\hat{t})} 1\,dx\,dy = M_0 \equiv \int\int_{D(0)} 1\,dx\,dy,$$
$$\int\int_{D_0(\hat{t})} (x,y)\,dx\,dy = \boldsymbol{M}_1 \equiv \int\int_{D(0)} (x,y)\,dx\,dy,$$

(the first moment $\boldsymbol{M}_1$ is just the position of the centre of mass times the area of the fluid domain) it follows from (9.1) that ∂D_0 is given at $\hat{t} \to \infty$ by the circle

$$|\boldsymbol{x} - \boldsymbol{M}_1/M_0|^2 = M_0/\pi,$$

with

$$\hat{p}_0 \to \sqrt{\pi/M_0}.$$

The second timescale is $t = O(1)$, with

$$p \sim \gamma\kappa_0(t) + p_0(x,y,t).$$

The boundary ∂D_0 remains circular, with radius

$$1/\kappa_0 = (M_0 + 2\pi Qt)^{1/2}/\pi^{1/2}$$

determined by the source strength and with origin determined by the exact conservation of first moment [33], giving $\partial D_0(t)$ to be

$$|\boldsymbol{x} - \boldsymbol{M}_1/(M_0 + 2\pi Qt)|^2 = (M_0 + 2\pi Qt)/\pi$$

(these three constraints on ∂D_0 can instead be obtained as solvability conditions on p_0). Blow-up thus occurs for $Q < 0$, with the moving boundary entering the sink at time

$$t = t_w \sim \left(M_0 - (\pi|\boldsymbol{M}_1|^2)^{1/3}\right)/(2\pi(-Q)).$$

No non-uniformity is readily apparent in the limit $t \to t_w^-$, providing important clues for the $\gamma = O(1)$ analysis which follows.

9.2 $\gamma = O(1)$: blow-up behaviour

Because p blows up only logarithmically as $r \to 0$, whereas κ scales with $1/r$, aspects of the large γ limit just described are of more general relevance in describing the behaviour at blow-up. Orienting the axes appropriately and assuming $\boldsymbol{M}_1 \neq \boldsymbol{0}$ (otherwise the problem is expected to become radially-symmetric as $t \to t_w^-$), the interface $\partial D(t)$ takes the form

$$x \sim \alpha(t_w - t) + o(y) \quad \text{as } t \to t_w^-,\ y \to 0$$

for some constant $\alpha > 0$, with

$$p(x,y,t_w) \sim -2Q\log r + p_c \quad \text{as } r \to 0,$$

https://doi.org/10.1017/S095679250400539X Published online by Cambridge University Press

where p_c is a constant, and

$$p(x,y,t) \sim -Q\log r - \frac{Q}{2}\log((x-2\alpha(t_w-t))^2+y^2) + p_c \tag{9.2}$$

as $t \to t_w^-$ with $x, y = O(t_w - t)$. It follows from (9.2) that the interface is given locally by

$$x \sim s(t) + \frac{Q}{\gamma}\left[\frac{1}{2}(y^2+\alpha^2(t_w-t)^2)\log(y^2+\alpha^2(t_w-t)^2) - \frac{3}{2}y^2 + 2\alpha(t_w-t)y\tan^{-1}\left(\frac{y}{\alpha(t_w-t)}\right)\right.$$
$$\left. - \alpha^2(t_w-t)^2\log(y^2+\alpha^2(t_w-t)^2) + \alpha^2(t_w-t)^2\log(\alpha(t_w-t))\right] - \frac{p_c}{2\gamma}y^2, \tag{9.3}$$

as $t \to t_w$, $y \to 0$, where $(s(t), 0)$ lies on ∂D with $s \sim \alpha(t_w - t)$ as $t \to t_w^-$, and

$$x \sim \frac{Q}{\gamma}\left(y^2\log y - \frac{3}{2}y^2\right) - \frac{p_c}{2\gamma}y^2$$

at $t = t_w$, $y \to 0$, so the curvature of the interface has a logarithmic singularity at the blow-up time; the effects of surface tension are thus sufficiently strong that ∂D is almost flat as it enters the sink. The values of α and p_c will depend upon γ and upon the initial data.

9.3 $\gamma \ll 1$: blow-up timescale

The scenario just described is not consistent with the wedge formation intermediate asymptotics of the ZST problem described earlier in the paper. For small γ there is thus a very short timescale with t close to t_w in which the local behaviour in the neighbourhood of the sink changes rather abruptly. It is clear from the self-similarity of the ZST solution that surface tension will enter only locally on the scales

$$t = t_w + \gamma^2 T, \quad \boldsymbol{x} = \gamma \boldsymbol{X}, \quad v_n = \gamma^{-1} V_N, \quad \kappa = \gamma^{-1} K,$$

with $T < 0$, and with leading order problem

$$\begin{gathered} \nabla^2 p_0 = 0, \\ p_0 = K_0, \quad \frac{\partial p_0}{\partial N} = -V_{0N} \quad \text{on } \partial D_0(T), \\ p_0 \sim -Q\log R \quad \text{as } R \to 0, \end{gathered} \tag{9.4}$$

where the initial data is imposed as $T \to -\infty$ in the form

$$p_0 \sim p_0\big(\boldsymbol{X}/(-T)^{1/2}\big)$$

(the ZST similarity solution), with ∂D_0 asymptoting in this limit (i.e. $T \to -\infty$ with $\boldsymbol{x} = O((-T)^{1/2})$) to the corresponding wedge. The local behaviour of (9.4) as $T \to 0^-$ is as described in § 9.2. The parameter Q can also be scaled out of (9.4), leaving (for given wedge angle) a parameter-free problem.

https://doi.org/10.1017/S095679250400539X Published online by Cambridge University Press

10 Discussion and conclusions

We have (re)constructed a family of solutions to the ZST Hele–Shaw free boundary problem which model the (apparently generic) intermediate asymptotic wedge-type blow-up behaviour of the NZST suction problem as observed in the numerics of Ceniceros *et al.* [8], Kelly & Hinch [28] and Nie & Tian [33]. These ZST solutions (which were first given by Ben Amar [2] in a different context as noted earlier) exist for any wedge angle (and any number of wedges), whereas the numerics suggest that a unique wedge angle is selected in the limit that the surface tension γ goes to zero. After studying the Schwarz function (1.1) that governs the evolution of solutions to the NZST Hele–Shaw problem, we hypothesised that a single member of our family of ZST solutions can be the limit of the NZST solution as $\gamma \to 0^+$: that for which the zero in the derivative of the Schwarz function is repeated. We claim that this is the unique solution that is selected in the limit $\gamma \to 0^+$.

Our claim is to be viewed as a conjecture; and in this sense its status is similar to that in which the Saffman–Taylor problem found itself for very many years. The problem we consider here is more delicate than that, since it is fully time-dependent. As with Saffman-Taylor, to some extent we must expect that what is selected will depend upon the chosen regularisation as mentioned in § 4.3. Nonetheless, we have a robust criterion, which we believe will be rather generally applicable.

We tested our criterion by comparison with the numerical results of [8]. We compared our hypothetical $N = 1$ critical solution with the local wedge-type behaviour displayed in Ceniceros *et al.* [8] and found a discrepancy between our calculated critical wedge angle (in the air) β_* and the converging table of wedge-angle values β_j given in Ceniceros *et al.* [8] for progressively smaller values of surface tension γ_j (Table II in Ceniceros *et al.* [8]). We thus compared the plots of tangent angle versus arclength for our solution and theirs (at surface tension $\gamma_2 = 4 \times 10^{-4}$) to see which angle, β_* or β_2, gave a better fit for the ZST solution. We believe that Figures 9 and 10 show our calculated critical angle β_* to give a much better fit. We attribute the discrepancy in numerical values of selected wedge angle to the ambiguity of 'wedge angle' for the non-idealised problem in which the geometry changes smoothly from the local inner wedge to the curved outer.

We also investigated the curvature of the wedge tip as blow-up is approached, which in the idealised ZST solution varies as the inverse square-root of time to wedge formation. The same self-similarity should also be found in the NZST calculations near blow-up time for $\gamma \ll 1$, and this appears to be the case in the numerics of Nie & Tian [8] for $\gamma_5 = 5 \times 10^{-5}$. We first used our ZST solution to calculate the constants of proportionality in the curvature law, both for our critical angle β_* and for the critical angle β_5 given in Ceniceros *et al.* [8] for γ_5. We then used the numerical results of Ceniceros *et al.* [8] to estimate the constant of proportionality independently, and found this estimate to lie almost exactly mid-way between the two values calculated for the two candidate critical angles. Hence this evidence favours neither critical angle over the other. Overall, however, we are satisfied that we have identified the correct critical angle.

We were also able to make some comparison between our analytical results over a large range of N-values and the numerical small-γ solutions carried out by Ben Amar

https://doi.org/10.1017/S095679250400539X Published online by Cambridge University Press

[3], and found our results to be very plausible as the ZST limit of the calculations carried out there.

We also note that, since our selection criterion depends only on knowledge of the ZST solution family, we expect it to provide the universal selection law, regardless of which regularisation is imposed. Preliminary numerical calculations have been carried out on the the Hele–Shaw suction problem subject to a kinetic undercooling regularisation at the interface [35, 38]. Unfortunately these computations are not taken sufficiently far to be able to observe wedge formation, and it would be very interesting to see more refined numerics carried out, to see if wedge formation (with the same critical angle) is observed here also. The Saffman–Taylor selection problem subject to a kinetic undercooling regularisation has been studied by Chapman & King [10], and in the limit that the kinetic undercooling regularisation goes to zero they again obtain the usual half-width finger, which may be traced back to the coincident singularities in the ZST problem.

The work of this paper and many others [16, 17, 18, 19, 24] demonstrates the utility of the P-K method in obtaining explicit analytical solutions to free boundary problems. Of course, the free boundary evolution of our ZST solution family could have been obtained numerically, probably much more easily than by the P-K method, and this is a frequent criticism of the method. However then we would not have been able to study the solution structure in the complex plane, and deduce the selection mechanism as we have done. For selection problems of this kind, methods such as the P-K one, which allow us to obtain analytical solutions, are extremely useful.

We mentioned in the Introduction the existence of similar numerical calculations carried out by Nie & Tian [34] for the case of a multipole driving singularity in the pressure, a situation for which one can also find explicit ZST solutions (though this problem has more than three singular points, which means that the standard P-K technique is not applicable, and the analysis is more complicated; see Craster [17] and Hoang & Craster [24]). However, all but one of the computations of Nie & Tian [34] are for $O(1)$ surface tension, so comparison with the $\gamma \to 0$ limit cannot be made; and the one computation made at small surface tension illustrates two fingers/wedges entering a dipole (Figure 8 in Nie & Tian [34]), whereas an exact ZST solution can only be written down for a single wedge entering a dipole. (Even could the relevant exact solution be written down, comparison with the single figure in Nie & Tian [34] would be impossible, since the local wedge geometry is strongly perturbed by the 'global' curvature of the free boundary.)

Finally, in § 2 the asymmetric wedge-type solutions of Tu [48] were mentioned. It would be an interesting (though computationally intensive) exercise to determine whether or not these solutions can ever be 'selected' according to our criterion.

Acknowledgements

We would like to thank Professor T. Y. Hou for his interest in our work, and in particular for his (and his co-authors') kind cooperation in providing us with the original figures and data from Ceniceros *et al.* [8]. LJC gratefully acknowledges financial support from an EPSRC Research Fellowship, and from a Royal Society Dorothy Hodgkin Research Fellowship, sponsored by National Grid.

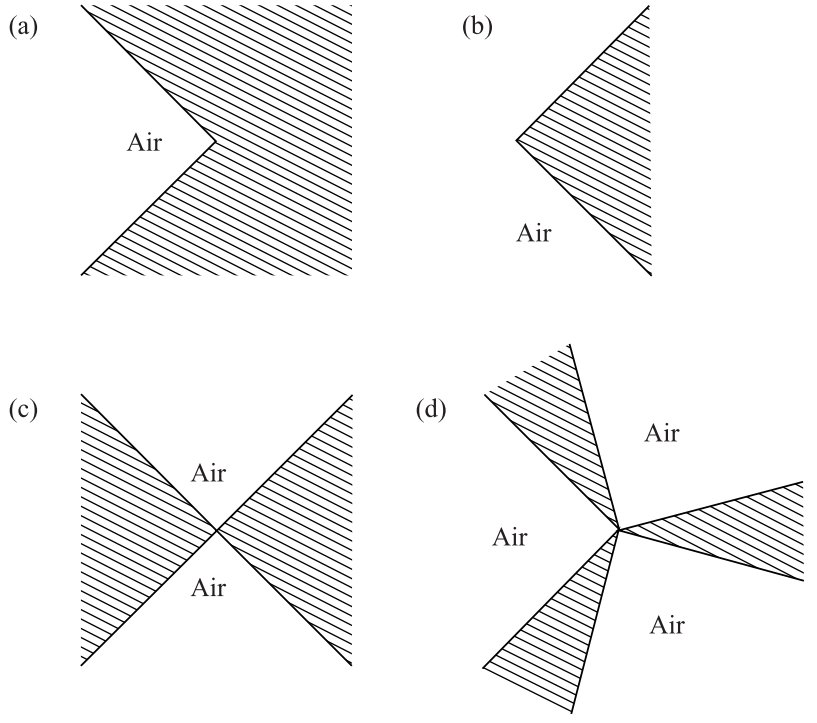

FIGURE A 1. The four special cases not covered by the solution (3.23).

Appendix A The special cases

The formula (3.23) giving the conformal map to the fluid region is not valid when $\frac{1}{2}+\frac{2}{\mu}=n\in\mathbb{N}$.[6] As stated after (3.23) earlier, there are four such possible ZST solutions, corresponding to the four cases in which the wedge angle in the air can be $\pi/2$ or $3\pi/2$. These configurations are indicated in figure A 1: $\mu=4/3$, $N=1$ (Figure A 1(a)); and $\mu=4$, with $N=1$, 2 or 3 (Figures A 1(b), (c) and (d)). The correct expression for $Z(\zeta)$ valid on $|\zeta|<1$ in these cases is provided by formula 15.3.14 in Abramowitz & Stegun [1]:

$$\begin{aligned}\mathscr{Z}(\zeta)=A_\infty e^{\frac{i\pi}{N}}\zeta^{-\frac{1}{N}}\Bigg\{&\frac{\Gamma\left(1+\frac{2}{N}\right)(-\zeta)^{\frac{1}{N}+\frac{n}{2}+\frac{1}{4}}}{\Gamma\left(\frac{1}{N}+\frac{n}{2}+\frac{1}{4}\right)\Gamma\left(\frac{1}{N}+\frac{n}{2}+\frac{3}{4}\right)}\\&\times\sum_{k=0}^{\infty}\frac{\left(\frac{1}{N}-\frac{n}{2}-\frac{1}{4}\right)_{k+n}\left(-\frac{1}{N}-\frac{n}{2}+\frac{1}{4}\right)_{k+n}}{k!(k+n)!}\zeta^k\times\Bigg[-\log(-\zeta)+\psi(1+n+k)\\&+\psi(1+k)-\psi\left(\frac{1}{N}+\frac{n}{2}+\frac{1}{4}+k\right)-\psi\left(\frac{1}{N}-\frac{n}{2}+\frac{3}{4}-k\right)\Bigg]\\&+(-\zeta)^{\frac{1}{N}-\frac{n}{2}+\frac{1}{4}}\frac{\Gamma\left(1+\frac{2}{N}\right)}{\Gamma\left(\frac{1}{N}+\frac{n}{2}+\frac{1}{4}\right)}\sum_{k=0}^{n-1}\frac{\Gamma(n-k)\left(\frac{1}{N}-\frac{n}{2}+\frac{1}{4}\right)_k}{k!\Gamma\left(\frac{1}{N}+\frac{n}{2}+\frac{3}{4}-k\right)}\Bigg\}\end{aligned}\tag{A 1}$$

[6] This corresponds to a special case in the Frobenius method of finding solutions to the ODE (3.19) (or (3.16)).

https://doi.org/10.1017/S095679250400539X Published online by Cambridge University Press

where A_∞ is as given in (3.22),

$$(a)_k \equiv a(a+1)\dots(a+k-1),$$

and $\psi(z) = d[\log(\Gamma(z))]/dz$ (the logarithmic derivative of the Gamma function, also known as Euler's psi function; see Abramowitz & Stegun [1] or Gradshteyn & Ryzhik [22]). Unfortunately, expression (A 1) does not appear to simplify to a closed form.

References

[1] Abramowitz, M. & Stegun, I. A. (1964) *Handbook of Mathematical Functions*. Dover.

[2] Ben Amar, M. (1991) Exact self-similar shapes in viscous fingering. *Phys. Rev. A*, **43**(10), 5724–5727.

[3] Ben Amar, M. (1991) Viscous fingering in a wedge. *Phys. Rev. A*, **44**(6), 3673–3685.

[4] Poire, E. C. & Ben Amar, M. (1998) Finger behaviour of a shear thinning fluid in a Hele–Shaw cell. *Phys. Rev. Lett*. **81**(10), 2048–2051.

[5] Ben Amar, M. & Poire, E. C. (1999) Pushing a non-Newtonian fluid in a Hele–Shaw cell: From fingers to needles. *Phys Fluids*, **11**(7), 1757–1767.

[6] Brener, E. A., Kessler, D. A., Levine, H. & Rappel, W.-J. (1990) Selection of the viscous finger in the 90° geometry. *Europhys. Lett*. **13**(2), 161–166.

[7] Carrier, G. F., Krook, M. & Pearson, C. E. (1966) *Functions of a Complex Variable*. McGraw-Hill.

[8] Ceniceros, H. D., Hou, T. Y. & Si, H. (1999) Numerical study of Hele–Shaw flow with suction. *Phys. Fluids*, **11**(9), 2471–2486.

[9] Chapman, S. J. (1999) On the role of Stokes lines in the selection of Saffman–Taylor fingers with small surface tension. *Euro. J. Appl. Math*. **10**, 513–534.

[10] Chapman, S. J. & King, J. R. (2003) The selection of Saffman-Taylor fingers by kinetic undercooling. *J. Eng. Math*. **46**(1), 1–32.

[11] Combescot, R., Hakim, V., Dombre, T., Pomeau, Y. & Pumir, A. (1986) Shape selection for Saffman–Taylor fingers. *Phys. Rev. Lett*. **56**, 2036–2039.

[12] Combescot, R., Hakim, V., Dombre, T., Pomeau, Y. & Pumir, A. (1988) Analytic theory of the Saffman-Taylor fingers. *Phys. Rev. A*, **37**(4), 1270–1283.

[13] Combescot, R. & Ben Amar, M. (1991) Selection of Saffman-Taylor fingers in the sector geometry. *Phys. Rev. Lett*. **67**(4), 453–456.

[14] Combescot, R. (1992) Saffman-Taylor fingers in the sector geometry. *Phys. Rev. A*, **45**(2), 873–884.

[15] Crank, J. (1984) *Free and Moving Boundary Problems*. Oxford University Press.

[16] Craster, R. V. (1994) Two related free boundary problems. *IMA Jl. Appl. Math*. **52**, 253–270.

[17] Craster, R. V. (1997) The solution of a class of free boundary problems. *Proc. R. Soc. Lond. A*, **453**, 607–630.

[18] Craster, R. V. & Hoang, V. H. (1998) Applications of Fuchsian differential equations to free boundary problems. *Proc. R. Soc. Lond. A*, **454**, 1241–1252.

[19] Cummings, L. J. (2000) Flow around a wedge of arbitrary angle in a Hele–Shaw cell. *Euro. J. Appl. Math*. **10**, 547–560.

[20] Elliott, C. M. & Janovsky, V. (1981) A variational inequality approach to Hele–Shaw flow with a moving boundary. *Proc. Roy. Soc. Edin*. **A88**, 93–107.

[21] Galin, L. A. (1945) Unsteady filtration with a free surface *Dokl. Akad. Nauk. S.S.S.R*. **47**, 246–249 (in Russian).

[22] Gradshteyn, I. S. & Ryzhik, I. M. (1980) *Table of Integrals, Series and Products* (corrected and enlarged edition). Academic Press.

[23] Hoang, Ha V., Hill, J. M. & Dewynne, J. N. (1998) Pseudo-steady-state solutions for solidification in a wedge. *IMA J. Appl. Math.* **60**, 109–121.
[24] Hoang, V. H. & Craster, R. V. (1998) Wedge solidification with differing types of boundary conditions. *IMA J. Appl. Math.* **67**, 509–524.
[25] Hong, D. C. & Langer, J. S. (1986) Analytic theory for the selection of Saffman–Taylor fingers. *Phys. Rev. Lett.* **56**, 2032–2035.
[26] Howison, S. D. & King, J. R. (1989) Explicit solutions to six free-boundary problems in fluid flow and diffusion. *IMA J. Appl. Math.* **42**, 155–175.
[27] Howison, S. D. (1992) Complex variable methods in Hele–Shaw moving boundary problems. *Euro. J. Appl. Math.* **3**, 209–224.
[28] Kelly, E. D. & Hinch, E. J. (1997) Numerical simulations of sink flow in the Hele–Shaw cell with small surface tension. *Euro. J. Appl. Math.* **8**, 533–550.
[29] King, J. R., Lacey, A. A. & Vazquez, J. L. (1995) Persistence of corners in free boundaries in Hele–Shaw flow. *Euro. J. Appl. Math.* **6**, 455–490.
[30] King, J. R. (1995) Development of singularities in some moving boundary problems. *Euro. J. Appl. Math.* **6**, 491–507.
[31] Lacey, A. A. (1982) Moving boundary problems in the flow of liquid through porous media. *J. Austral. Math. Soc.* **B24**, 171–193.
[32] McLean, J. W. & Saffman, P. G. (1981) The effect of surface tension on the shape of fingers in a Hele–Shaw cell. *J. Fluid Mech.* **102**, 445–469.
[33] Nie, Q. & Tian, F. R. (1998) Singularities in Hele–Shaw flows. *S.I.A.M. J. Appl. Math.* **58**(1), 34–54.
[34] Nie, Q. & Tian, F. R. (2001) Singularities in Hele–Shaw flows driven by a multipole. *S.I.A.M. J. Appl. Math.* **62**(2), 385–406.
[35] Pleshchinskii, N. B. & Reissig, M. (2002) Hele–Shaw flows with nonlinear kinetic undercooling regularisation. *Nonlinear Anal.* **50**, 191–203.
[36] Polubarinova-Kochina, P. Ya. (1945) On the motion of the oil contour. *Dokl. Akad. Nauk. S.S.S.R.* **47**, 254–257 (in Russian).
[37] Polubarinova-Kochina, P. Ya. (1962) *Theory of Groundwater Movement*. Princeton University Press.
[38] Reissig, M., Rogosin, S. V. & Hübner, F. (1999) Analytical and numerical treatment of a complex model for Hele–Shaw moving boundary problems with kinetic undercooling regularization. *Euro. J. Appl. Math.* **10**, 561–579.
[39] Richardson, S. (1972) Hele–Shaw flows with a free boundary produced by the injection of fluid into a narrow channel. *J. Fluid Mech.* **56**, 609–618.
[40] Richardson, S. (2001) Hele–Shaw flows with free boundaries in a corner or around a wedge Part I: Liquid at the vertex. *Euro. J. Appl. Math.* **12**(6), 665–676.
[41] Richardson, S. (2001) Hele–Shaw flows with free boundaries in a corner or around a wedge Part II: Air at the vertex. *Euro. J. Appl. Math.* **12**(6), 677–688.
[42] Saffman, P. G. & Taylor, G. I. (1958) The penetration of a fluid into a porous medium or Hele–Shaw cell containing a more viscous liquid. *Proc. Roy, Soc. Lond. A*, **245**, 312–329.
[43] Shraiman, B. I. (1986) Velocity selection and the Saffman-Taylor problem. *Phys. Rev. Lett.* **56**, 2028–2031.
[44] Siegel, M. & Tanveer, S. (1996) Singular perturbation of smoothly evolving Hele–Shaw solutions. *Phys. Rev. Lett.* **76**(3).
[45] Siegel, M., Tanveer, S. & Dai, W.-S. (1996) Singular effects of surface tension in Hele–Shaw cells. *J. Fluid Mech.* **323**, 201–236.
[46] Tanveer, S. (2000) Surprises in viscous fingering. *J. Fluid Mech.* **409**, 273–308.
[47] Thomé, H., Rabaud, M., Hakim, V. & Couder, Y. (1989) The Saffman-Taylor instability: From the linear to the circular geometry. *Phys. Fluids A*, **1**, 224–240.
[48] Tu, Y. (1991) Saffman-Taylor problem in sector geometry: Solution and selection. *Phys. Rev. A*, **44**(2), 1203–1210.
[49] van Dyke, M. (1975) *Perturbation Methods in Fluid Mechanics*. Parabolic Press.